Calibration of Magnetic Distortions in the LHCb-RICH1 Photon Detectors

Fatima Soomro

Imperial College
London

The LHCb Detector

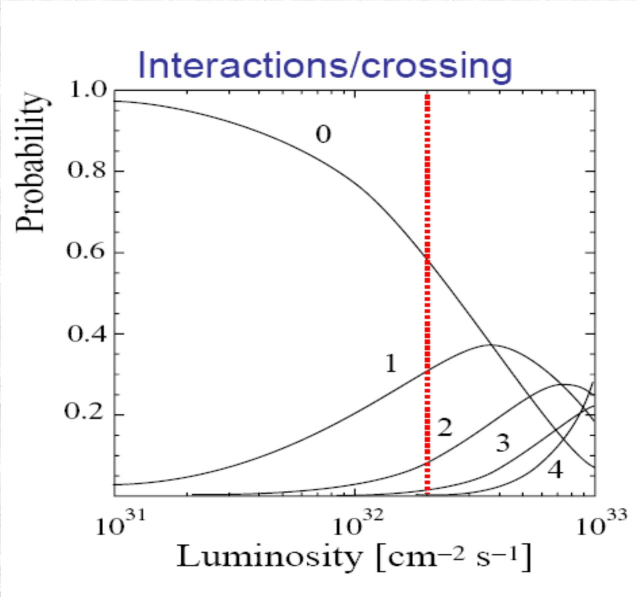

b bbar Cross section = 500 μb
10^{12} b bbar pairs in one year

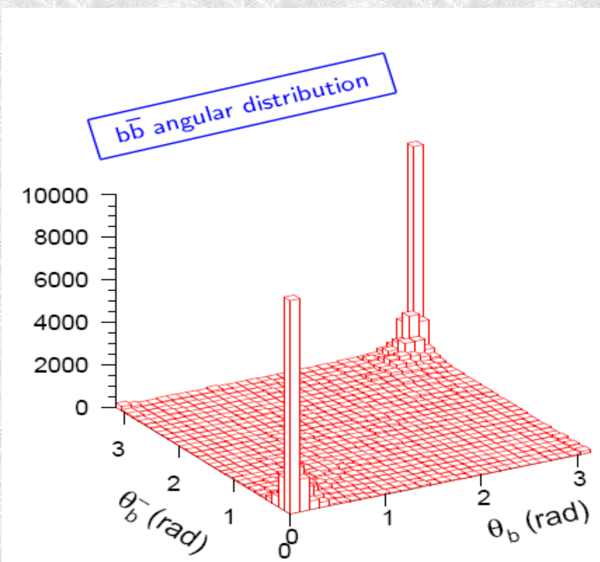

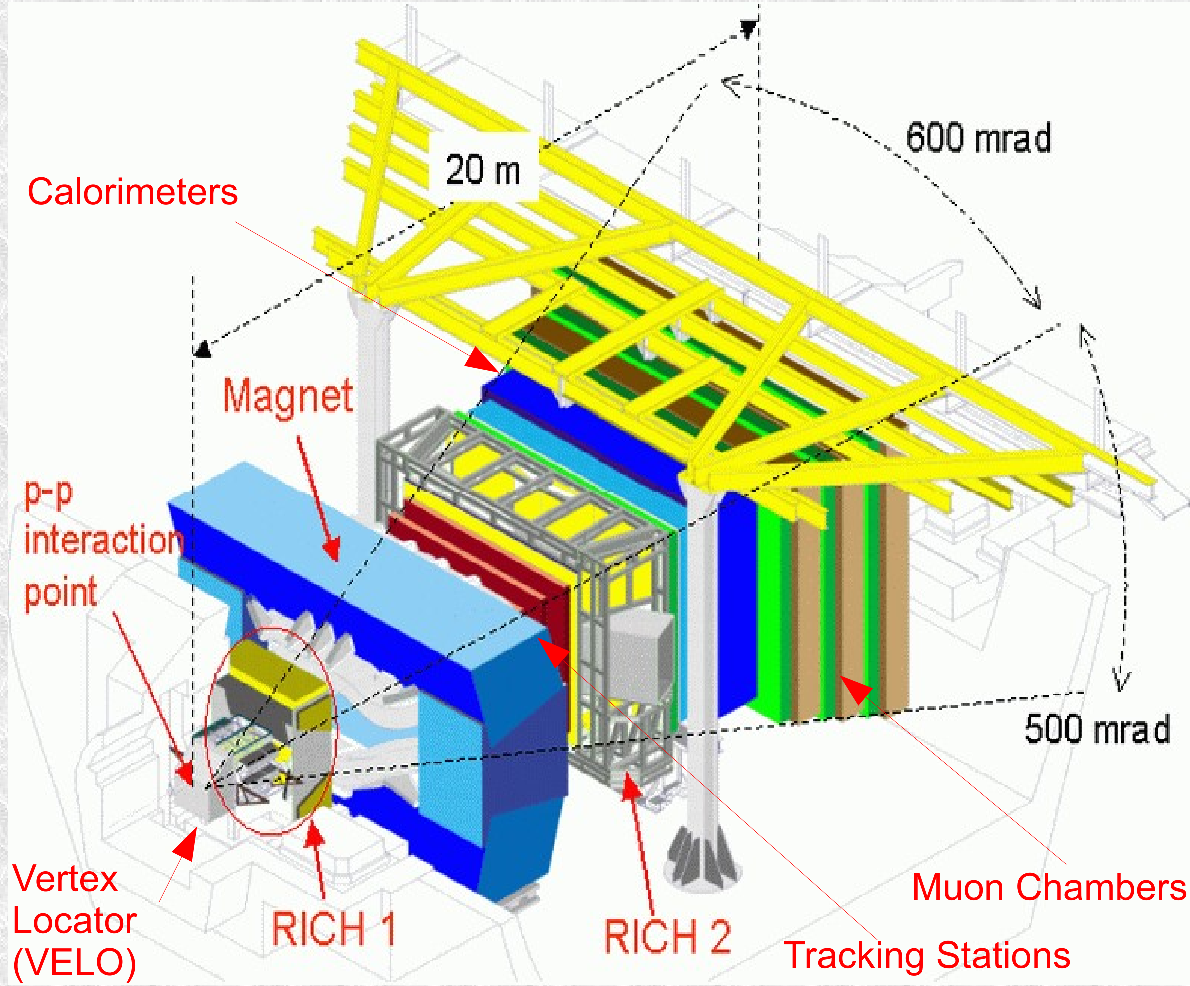

A Single-arm spectrometer for

- **precision measurements of CP violation in B-hadrons**
- **search for new physics in rare b decays**

Ring Imaging Cherenkov (RICH) Detectors for Particle Identification (PID) in LHCb:

RICH1:
upstream of the magnet.
momentum range:
~2-60 GeV/c
radiators: Aerogel, n=1.03, L=5 cm
C_4F_{10} ,n=1.0014, L= 95 cm

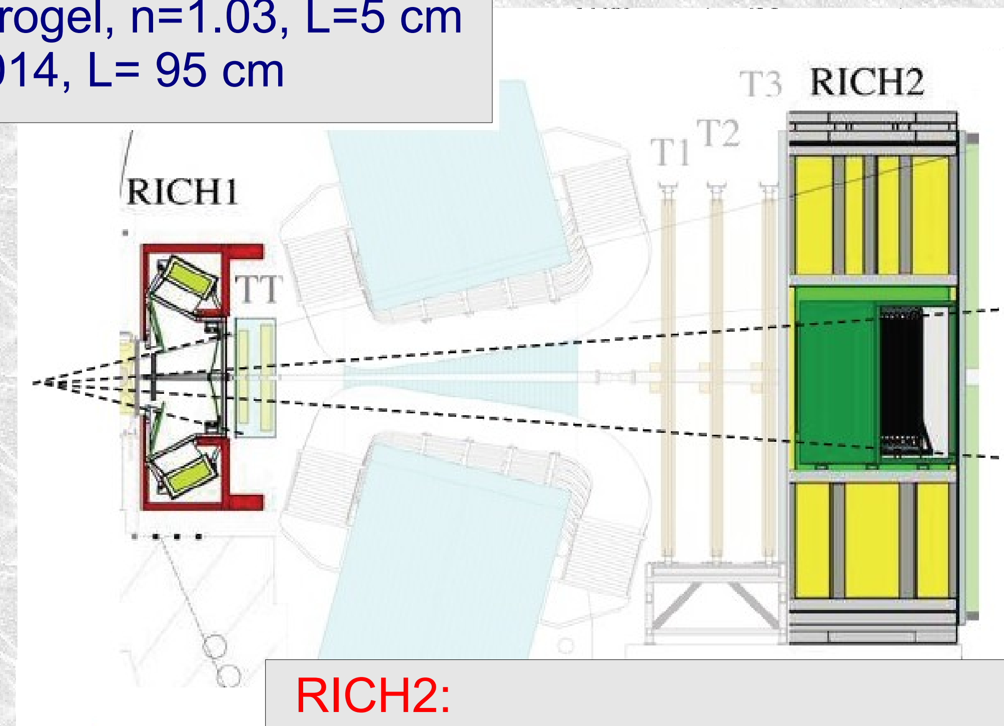

RICH2:
downstream of the magnet
momentum range 60 to
beyond 100 GeV/c
radiator: CF_4, n=1.0005, L=180 cm

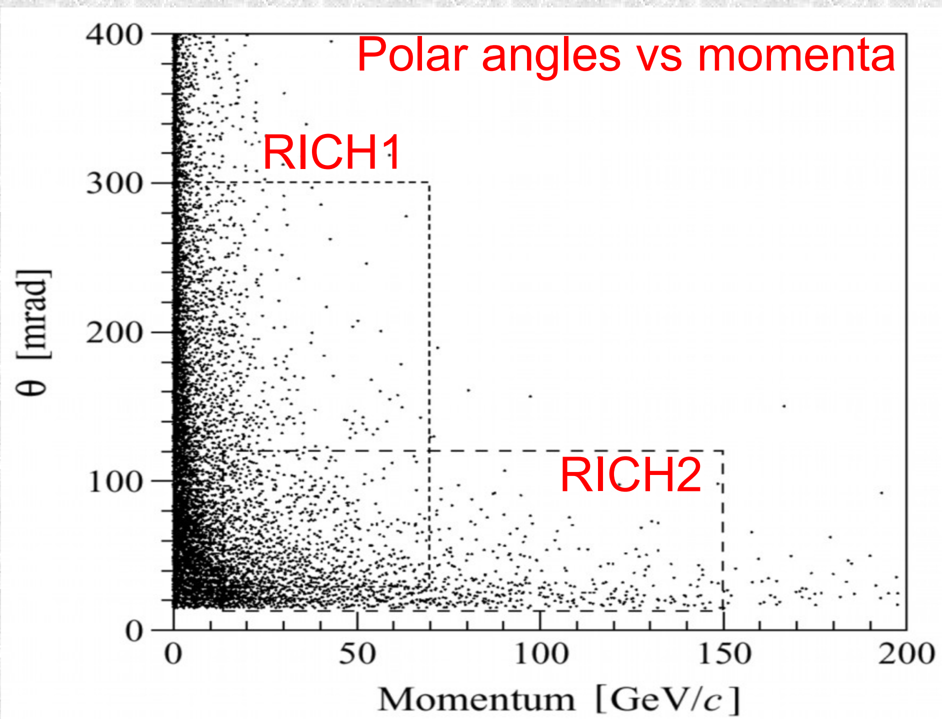

Imperial College
London

Working Principle: Cherenkov Radiation

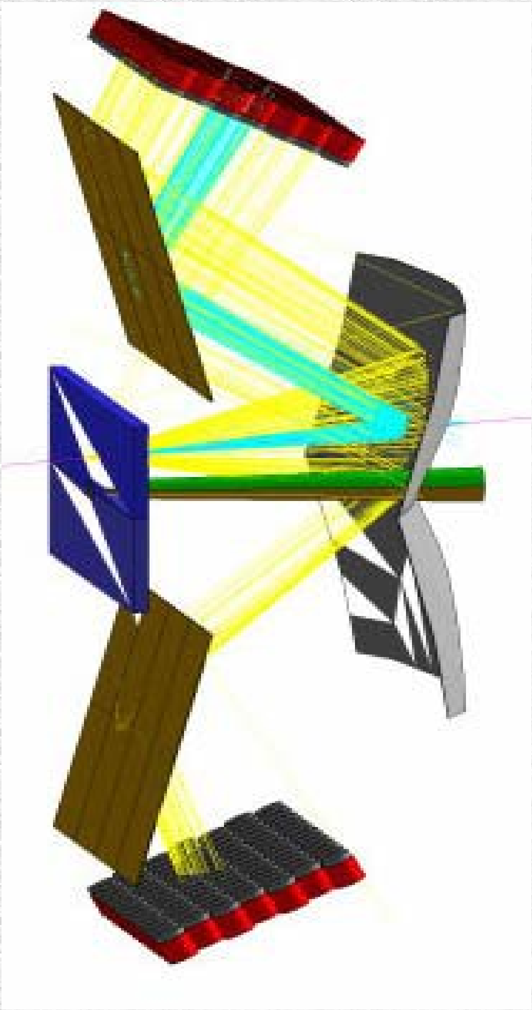

A charged particle travelling in a medium, at a speed faster than the speed of light in that medium, emits Cherenkov Photons.

$$\cos \theta_c = 1/ n\beta$$

Speed of the charged particle β

Opening angle of the cone of Cherenkov Photons θ_c

Refractive index of the medium n

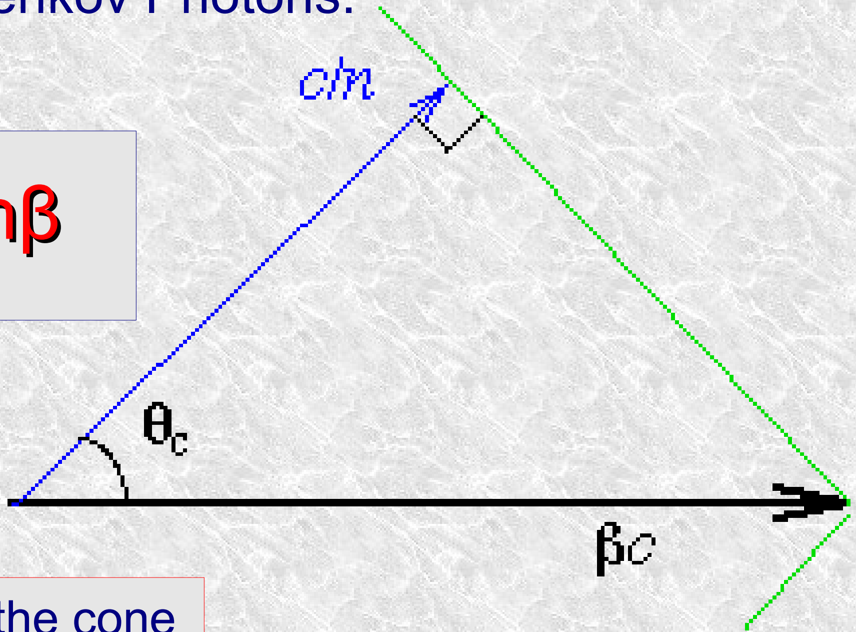

The RICH1 Detector

The RICH1 design was motivated by the following considerations:

- Available space
- Minimize material within acceptance
- Access to beam pipe

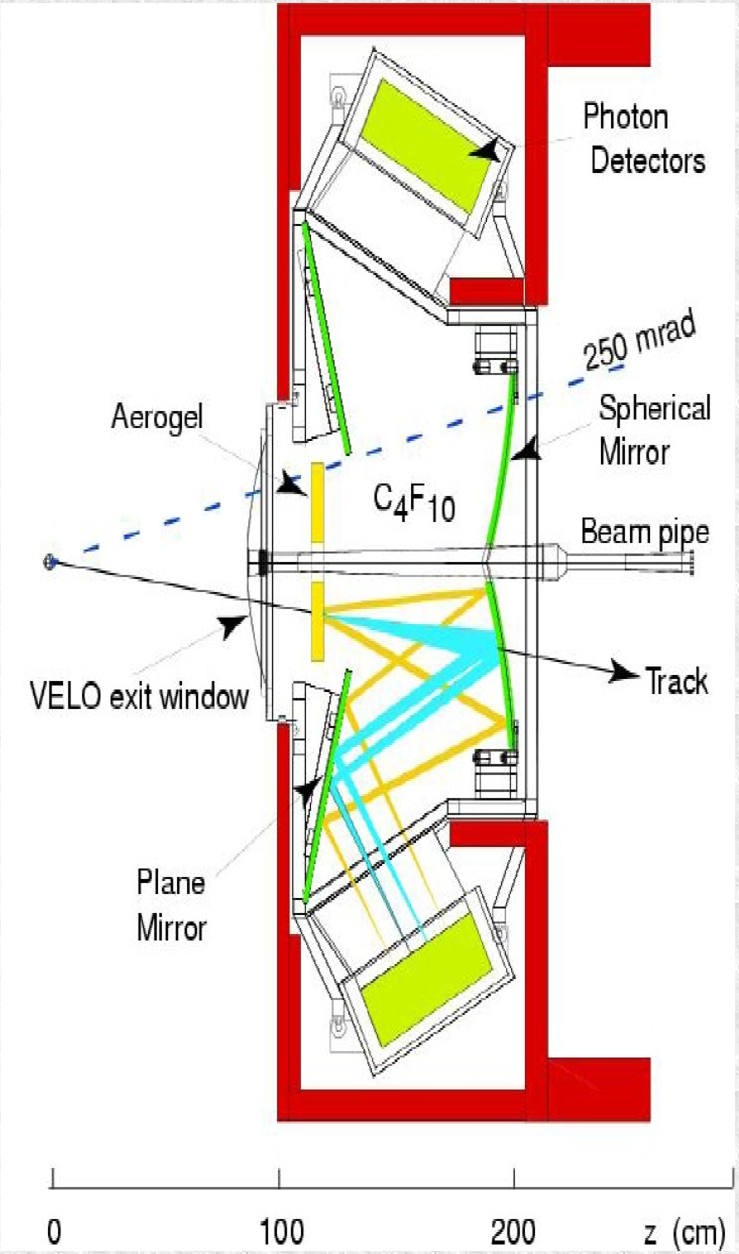

Photon Detectors for the RICH Detectors:

The Requirements

The Choice

Pixel Hybrid photon

Detectors (HPDs)

- High Quantum efficiency
- High granularity 2.5 x 2.5 mm^2
- High active to total area
  64% after close packing
- Good signal to noise ratio
- Single photoelectron
  detection efficiency ~85%
- Readout compatible with 25 ns
  bunch crossing of LHC
- Operable in magnetic field
  - B < 50 Gauss
  - local shielding
  - offline correction
- Withstand radiation dose of 3kRad/yr
  ability demonstrated

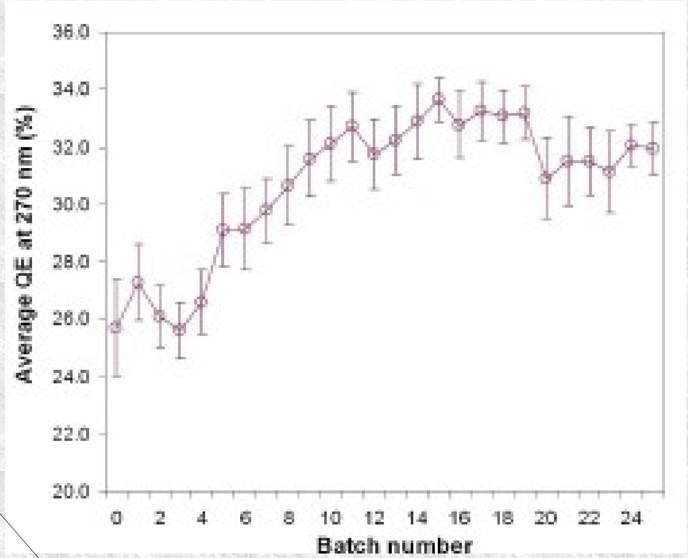

signal 5000 e
noise 160 e
Threshold 1200 e
(RMS spread 100e)

The HPD – Internal structure and Working

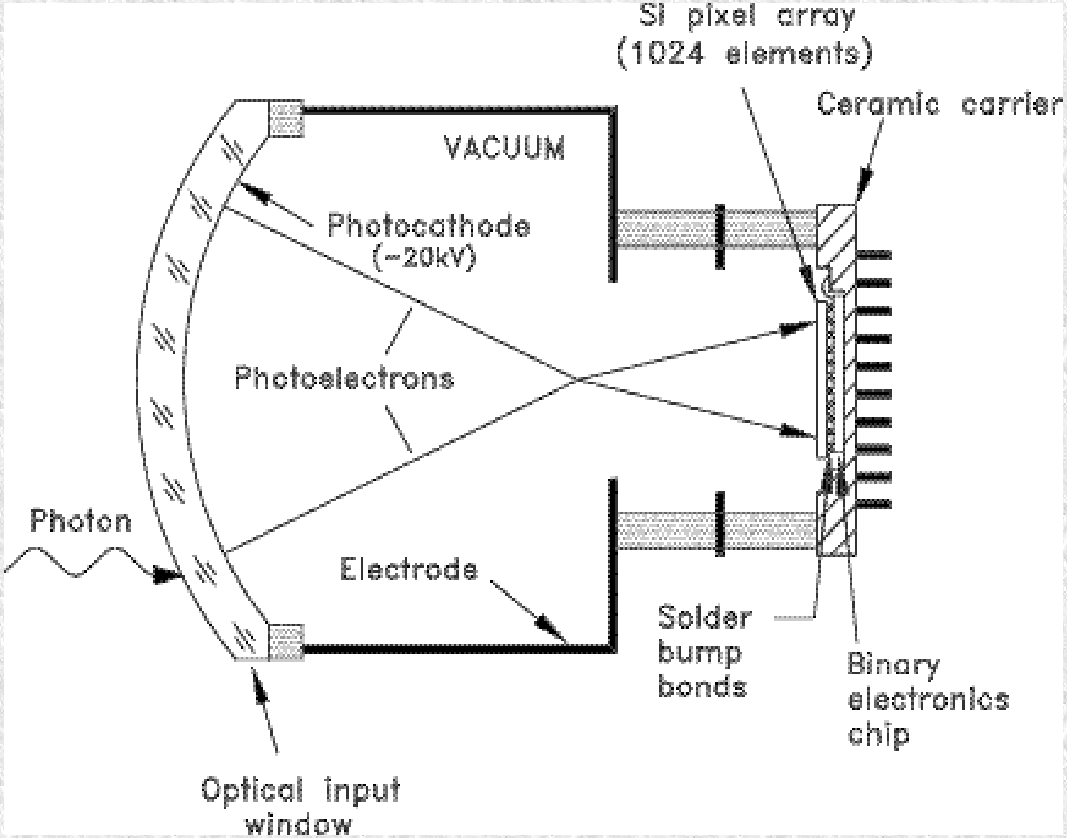

- Vacuum tube
- Quartz window
- S20 multi-alkali photocathode(-20 kV)
- Cross focusing electron optics
- Si pixel anode at ground (1024 elements)
- Pixel anode bump bonded to readout chip.

The HPD – Internal structure and Working

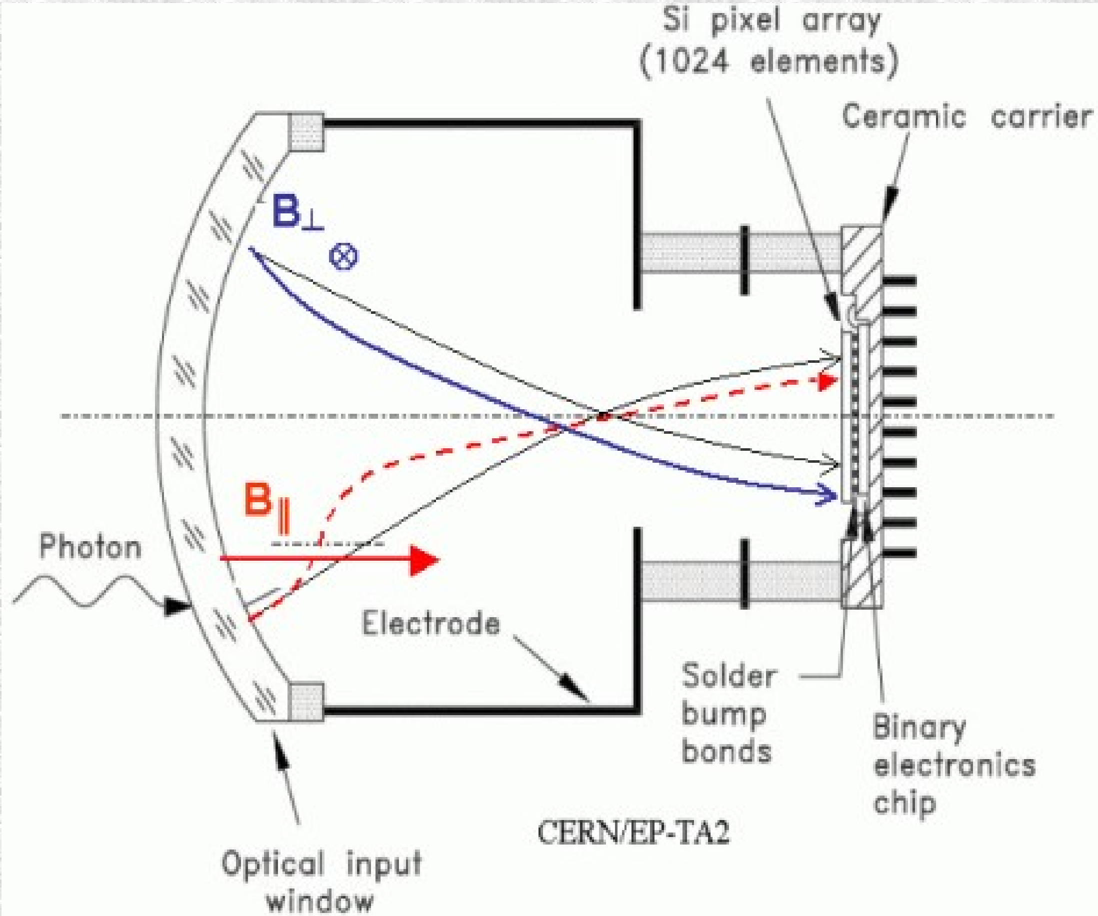

- Vacuum tube
- Quartz window
- S20 multi-alkali photocathode(-20 kV)
- Cross focusing electron optics
- Si pixel anode at ground (1024 elements)
- Pixel anode bump bonded to readout chip.

Imperial College
London

Test pattern measurements with locally shielded HPD

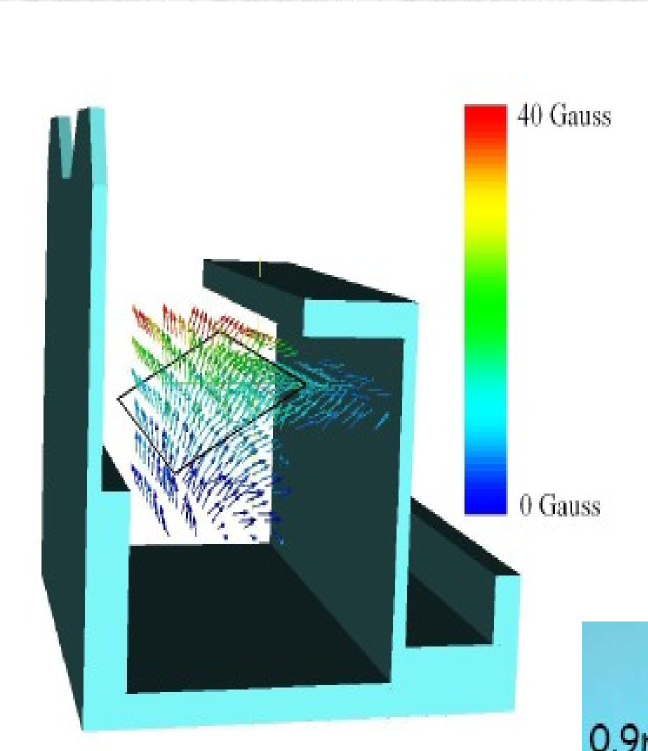

The magnetic field at the HPD plane and Local Shielding for the HPDs.

Notice that the Magnetic field is not uniform and varies from tube to tube.

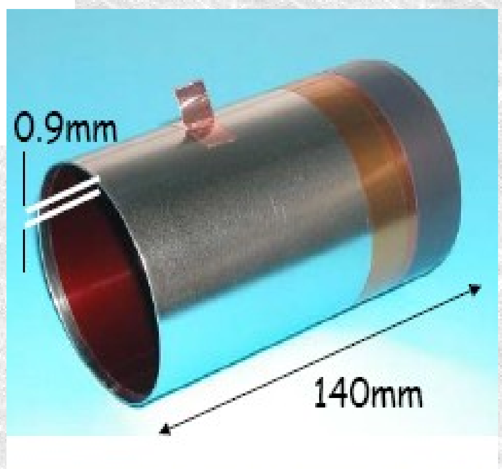

Mu-metal shield grounded and insulated with ~250μm-thick Kapton foil

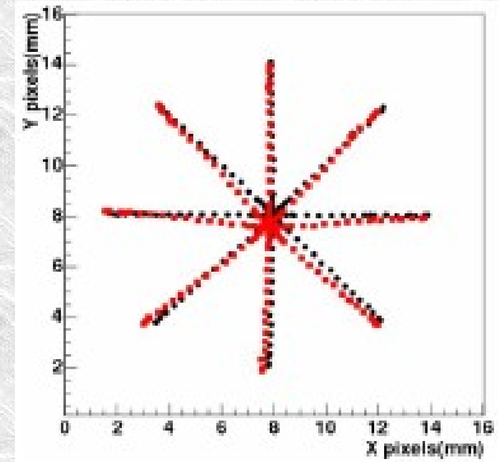

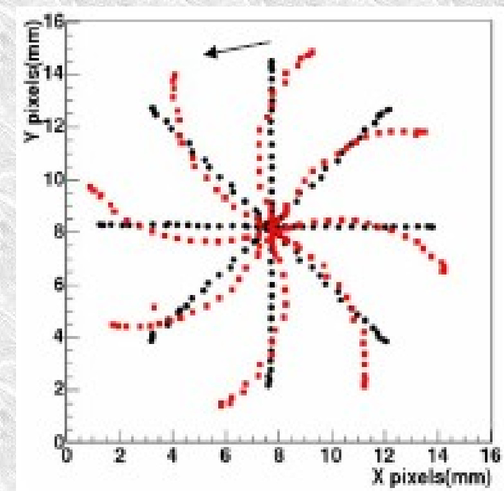

Distortion patterns for 50 Gauss transverse field (top) and 50 Gauss axial field, overlapped with the reference 0 Gauss image.

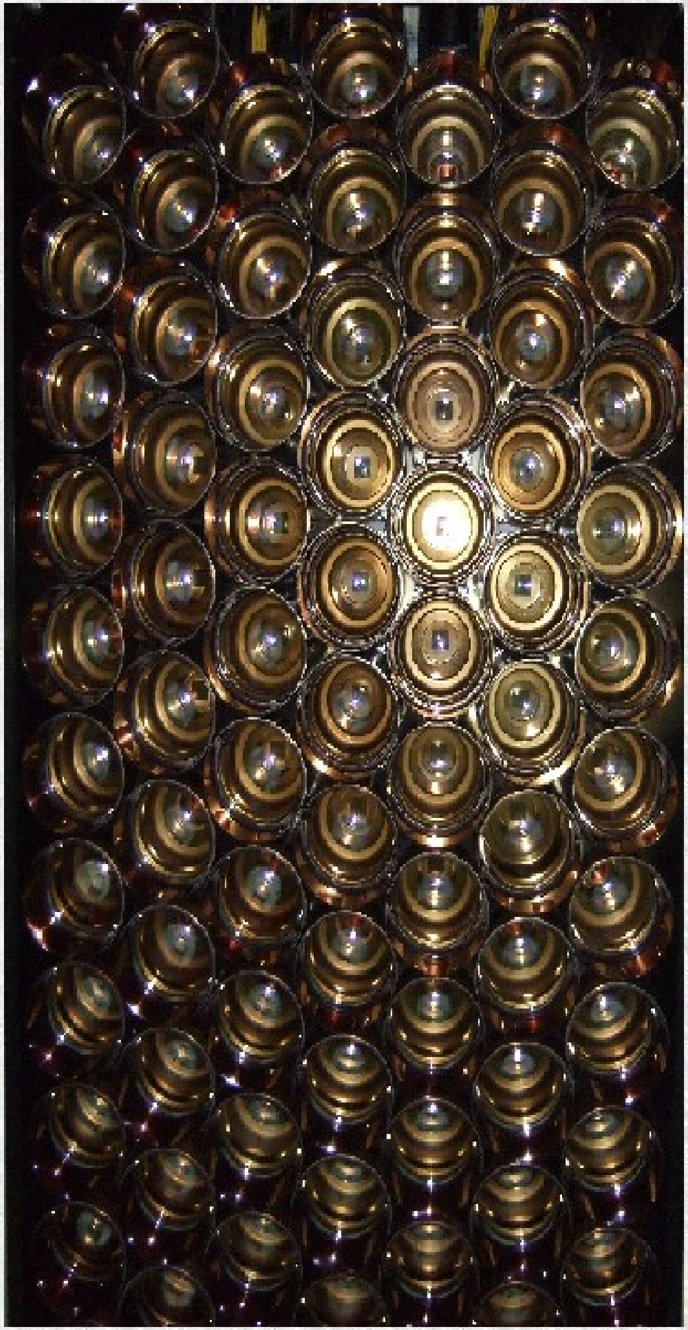

Characterizing the magnetic distortion (My Future Work)

- Scan a collimated light source over the entire HPD plane.
- Find a relationship between the position of light source on the HPD window and the signal on Si anode.
- Develop a map or look up table.

The magnetic distortion system

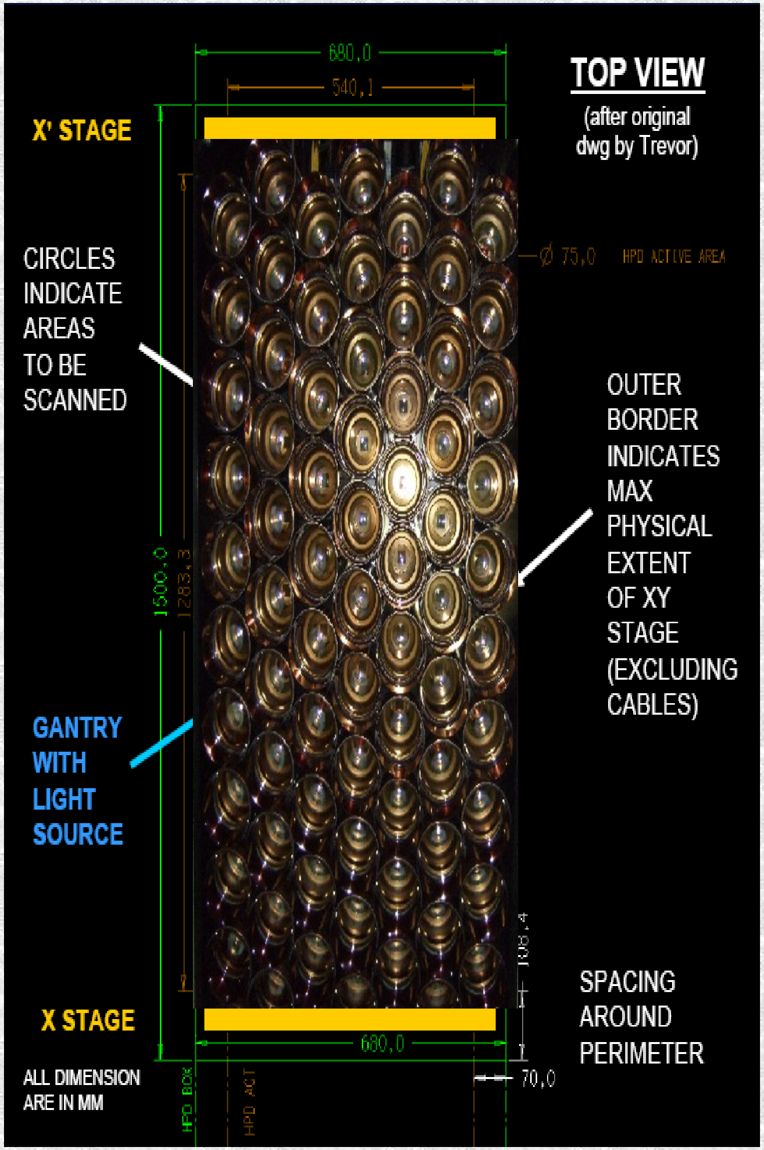

The magnetic distortion system

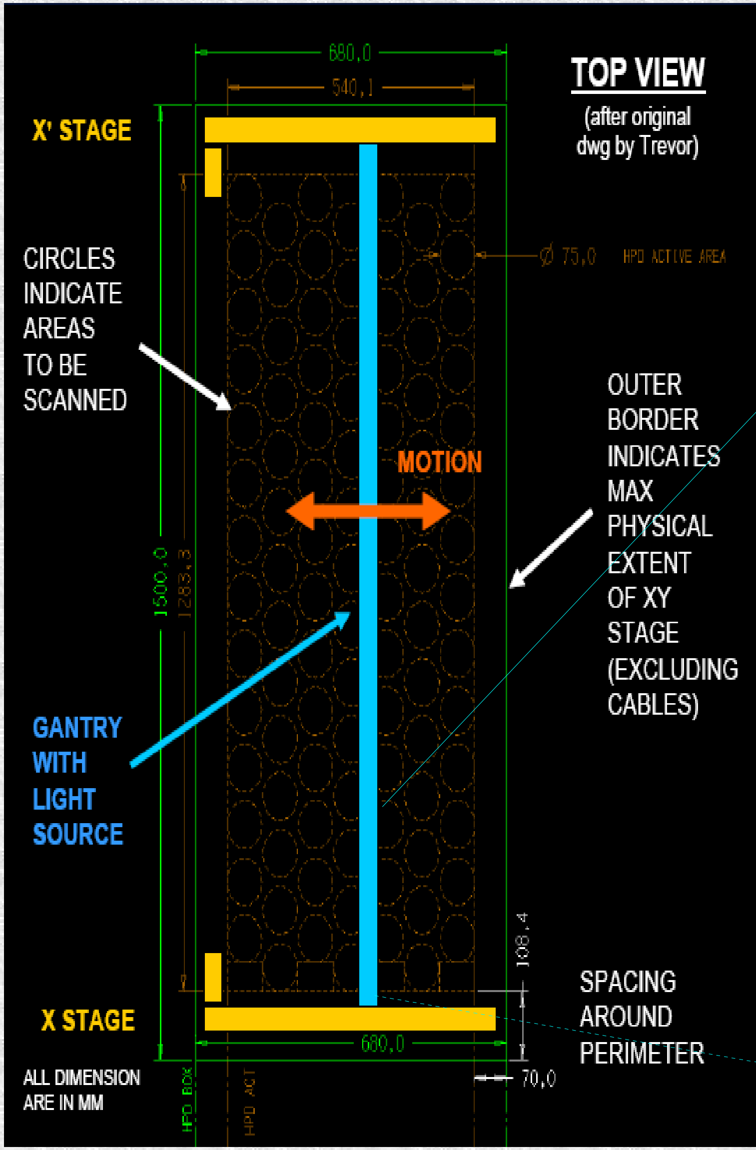

The LED matrix

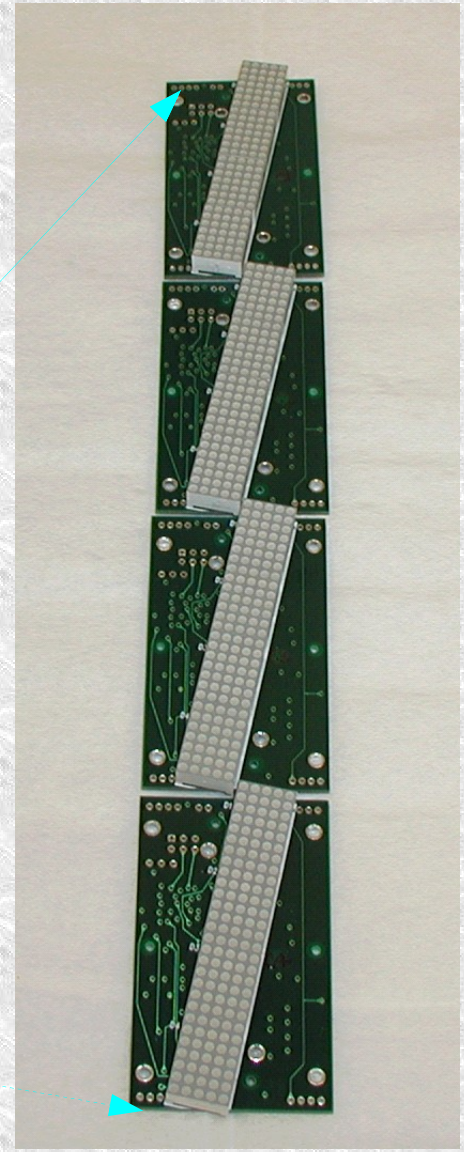

A calculation assuming the LED to emit photons at a rate of 1Mhz shows that to scan the entire HPD plane with a resolution of 0.5 mm^2 will take 6 months!!

It is very important to develop a strategy and pattern, which has an adequate resolution and is less time consuming.

Conclusion and current status

- **The HPDs are extremely elegant photon detectors providing**
  - *good quantum efficiency*
  - *good signal to noise*
  - *excellent resolution*
- **Their operating conditions in LHCb:** *not optimal*
- **Performance can be restored with**
  - *local shielding*
  - *calibration*
  - *offline correction*

- **The distortion system is in advance stages of manufacture and will be delivered to CERN around Easter.**
- **The DAQ and analysis software is yet to be written.**

Spare slides

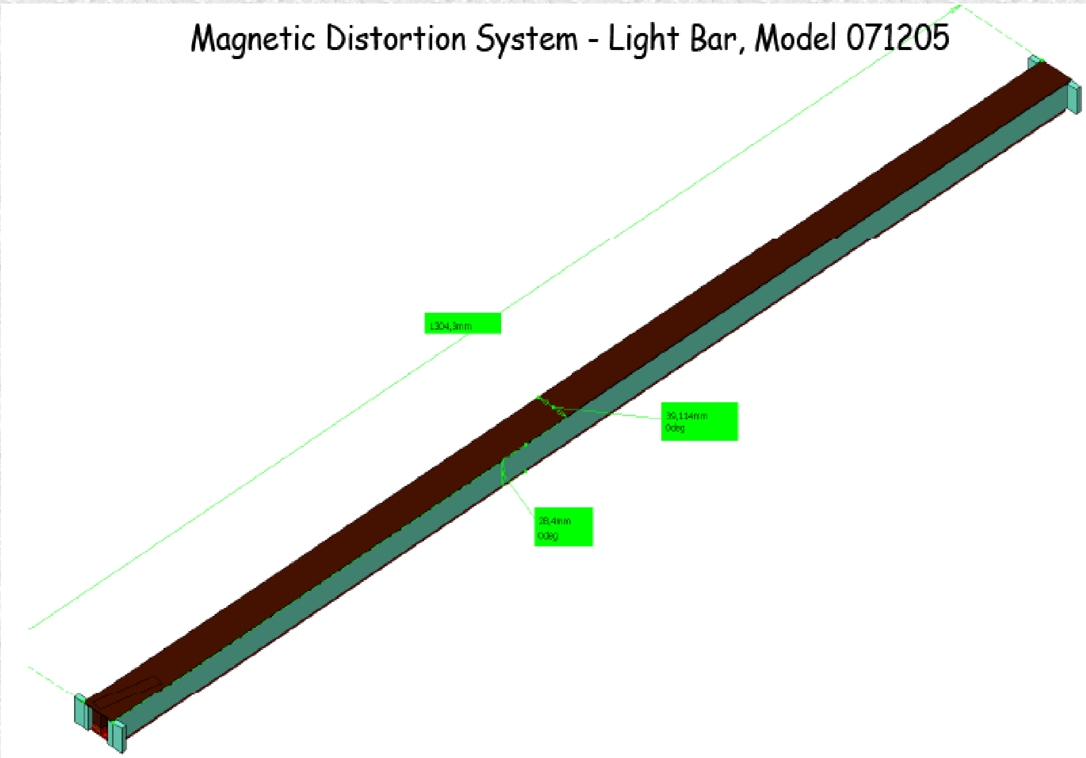
Magnetic Distortion System - Light Bar, Model 071205
1304,3mm
39,114mm
0deg
28,4mm
0deg

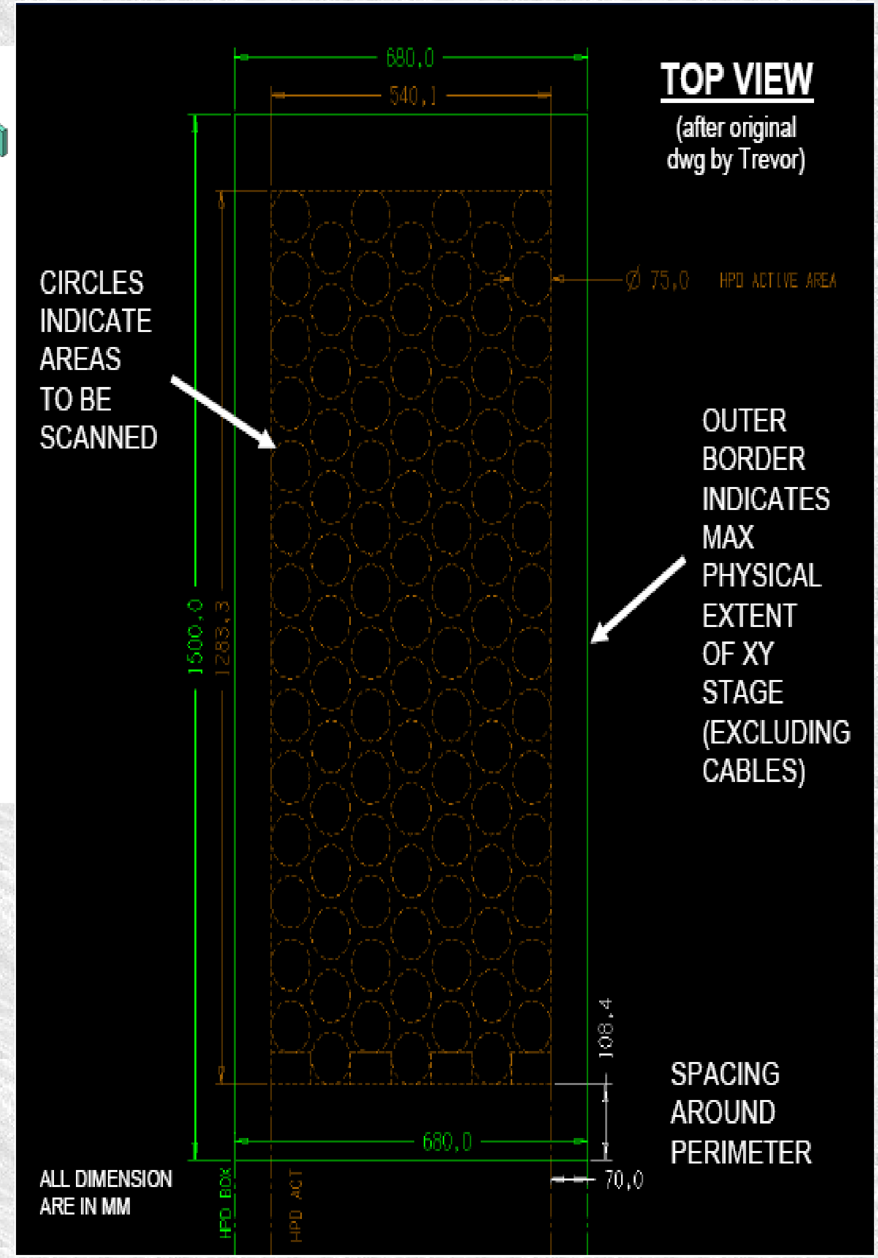
TOP VIEW
(after original dwg by Trevor)
680,0
540,1
CIRCLES INDICATE AREAS TO BE SCANNED
Ø 75,0
HPD ACTIVE AREA
OUTER BORDER INDICATES MAX PHYSICAL EXTENT OF XY STAGE (EXCLUDING CABLES)
1500,0
1283,3
108,4
SPACING AROUND PERIMETER
680,0
70,0
ALL DIMENSION ARE IN MM
HPD BOX
HPD ACT

Particle Identification (PID) in LHCb: Ring Imaging Cherenkov (RICH) Detectors

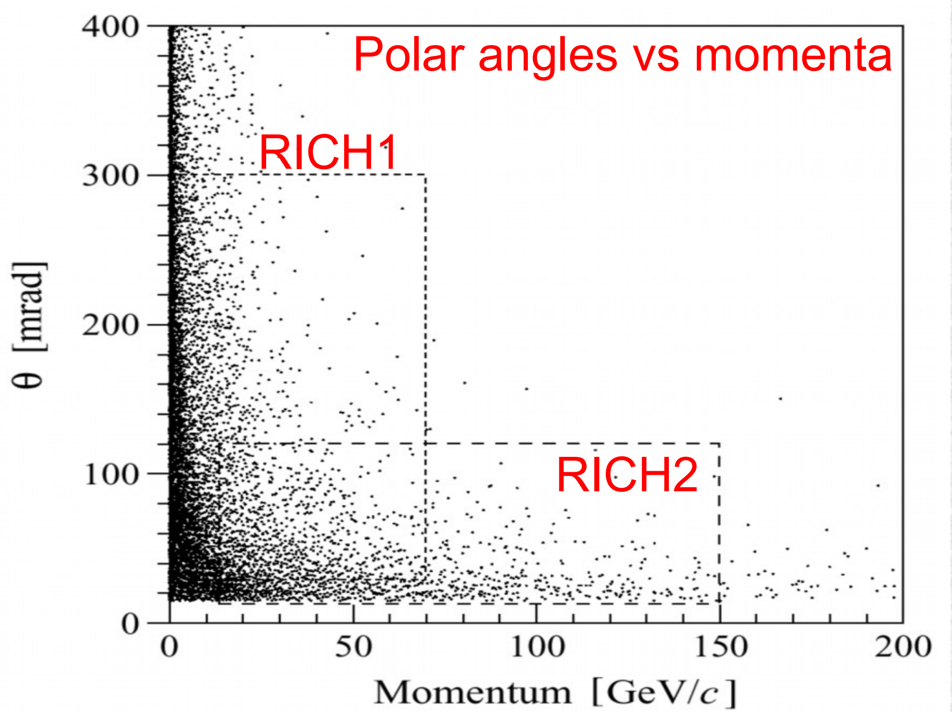

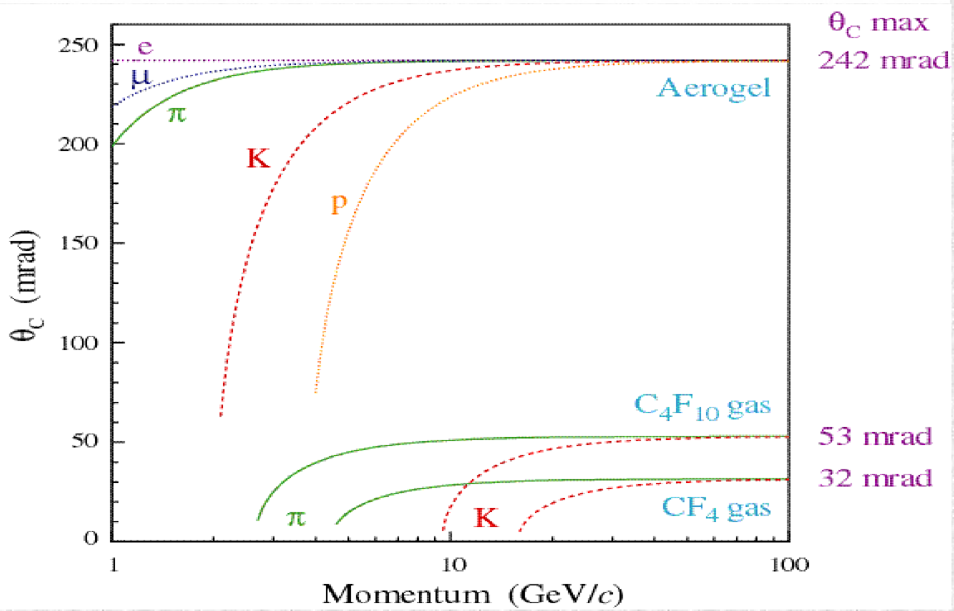

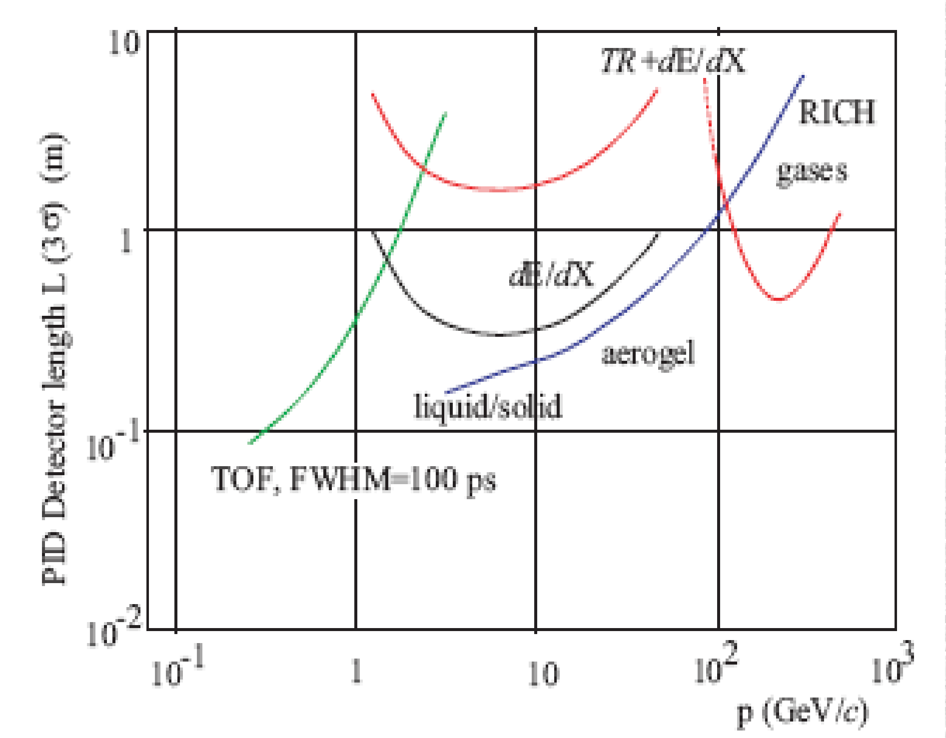

π/K Separation by different PID methods

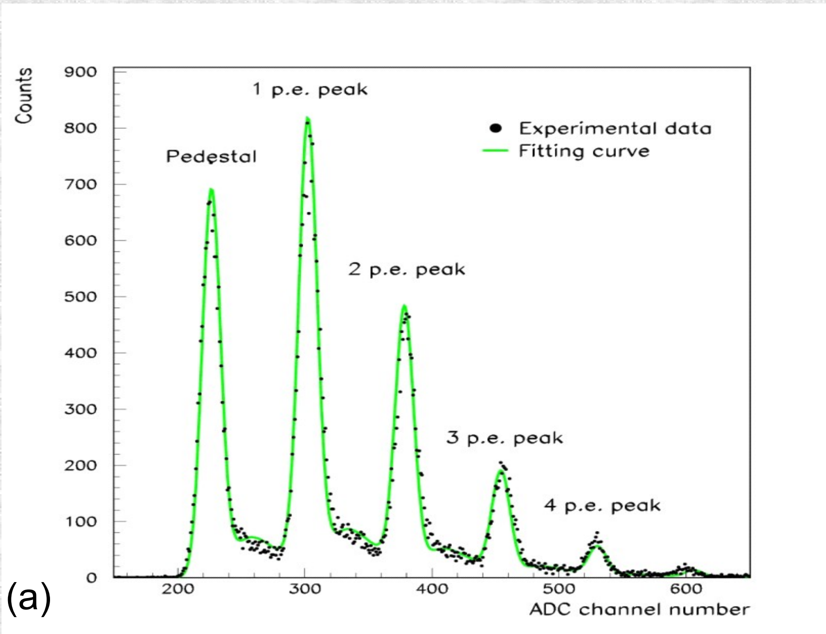

(a)

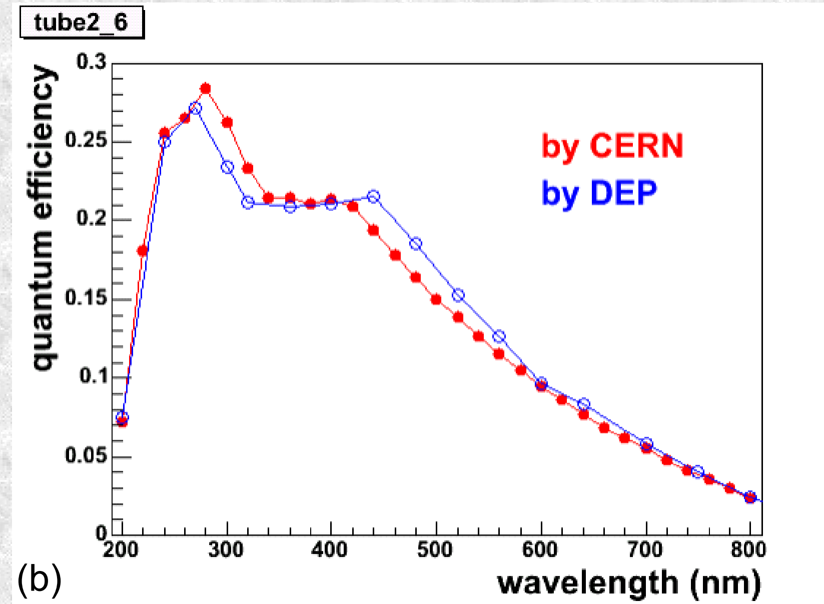

(b)

(a) Response curve shows excellent signal to noise separation

(b) QE of a single HPD

(c)The average QE(%) at 270 nm versus the HPD batch number

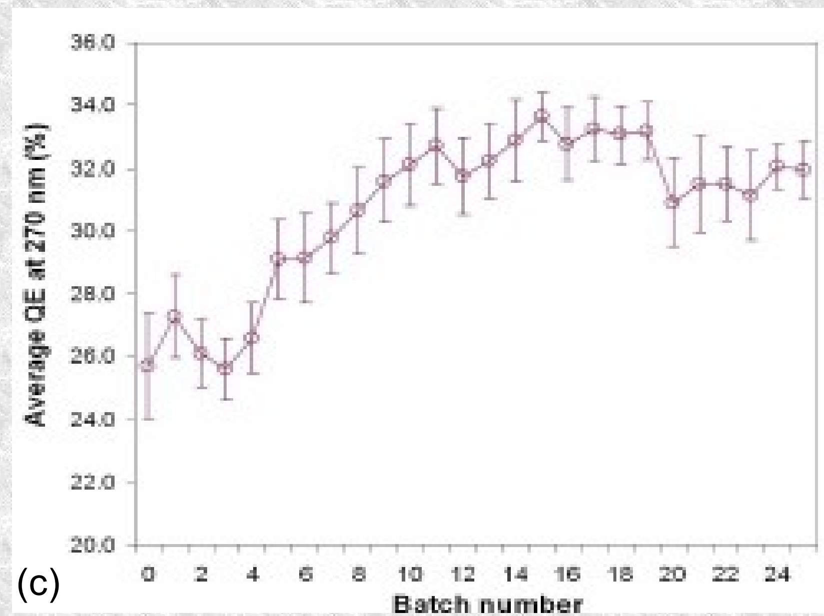

(c)

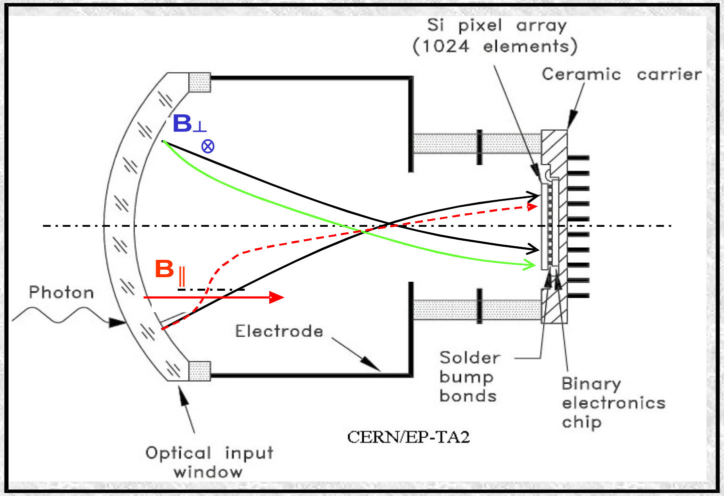

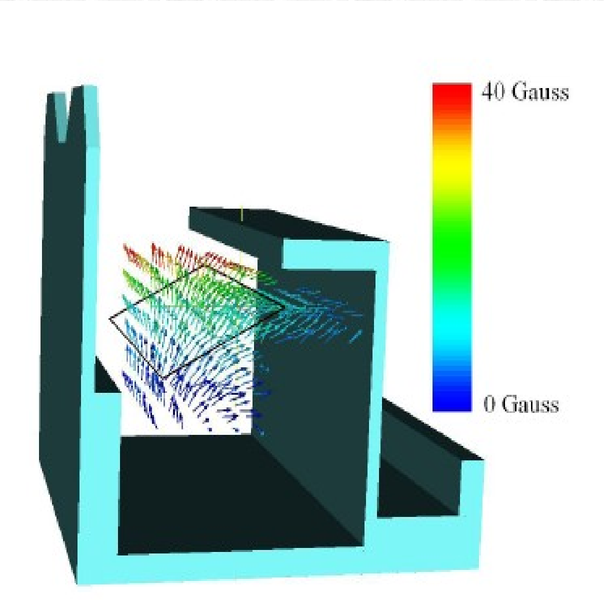

The field vectors around the HPD plane and under the internal shelf.

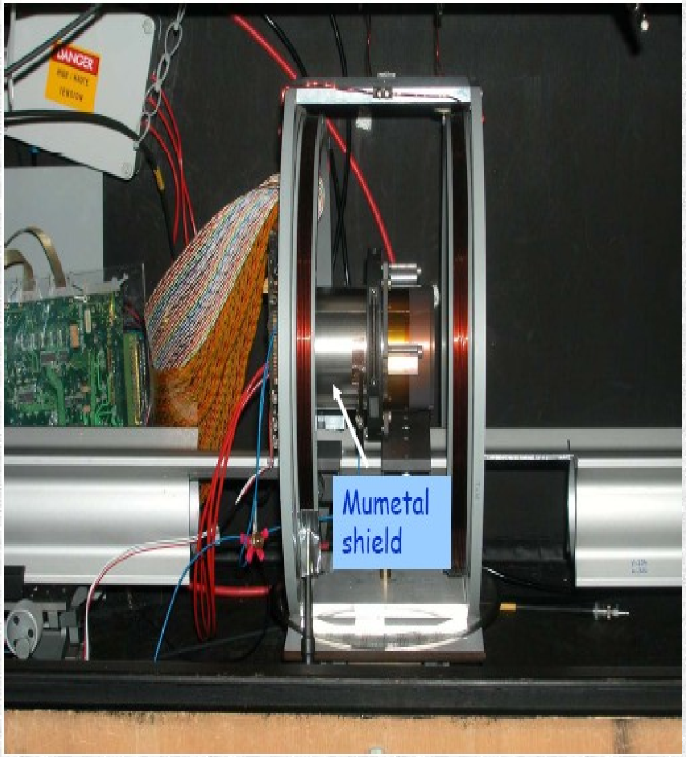

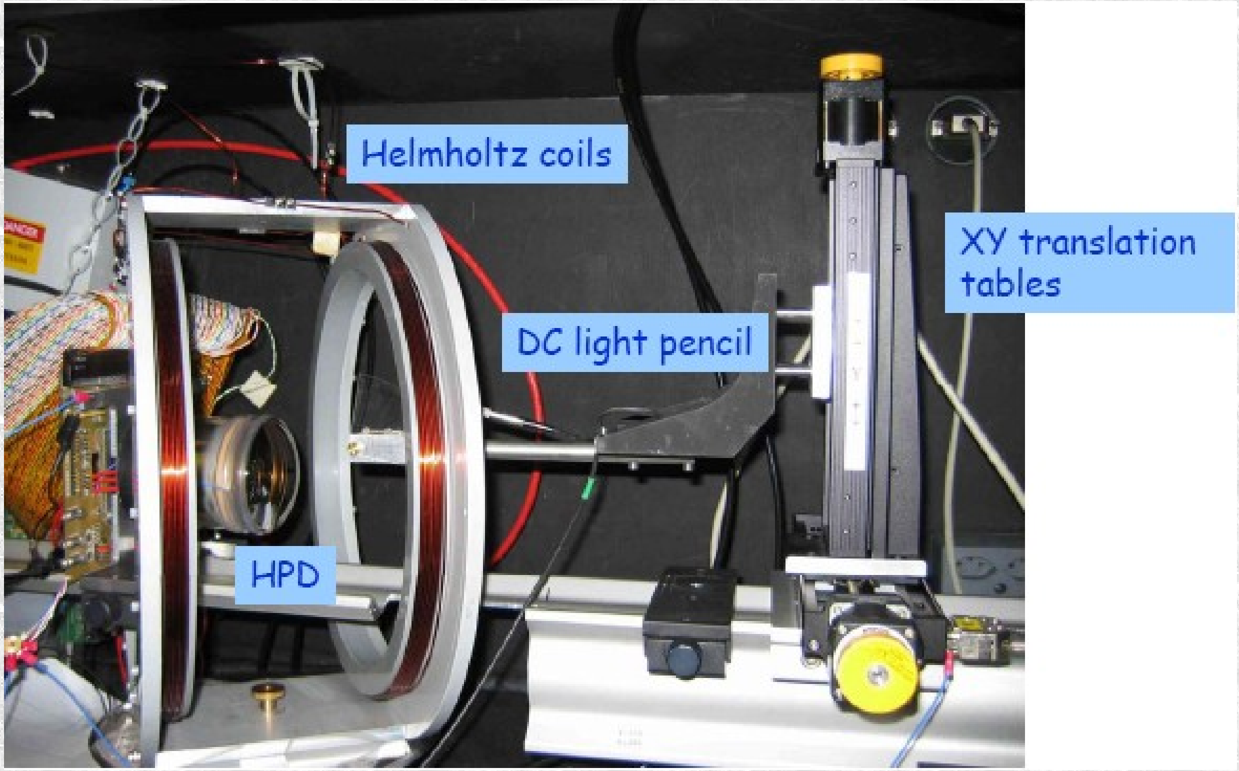

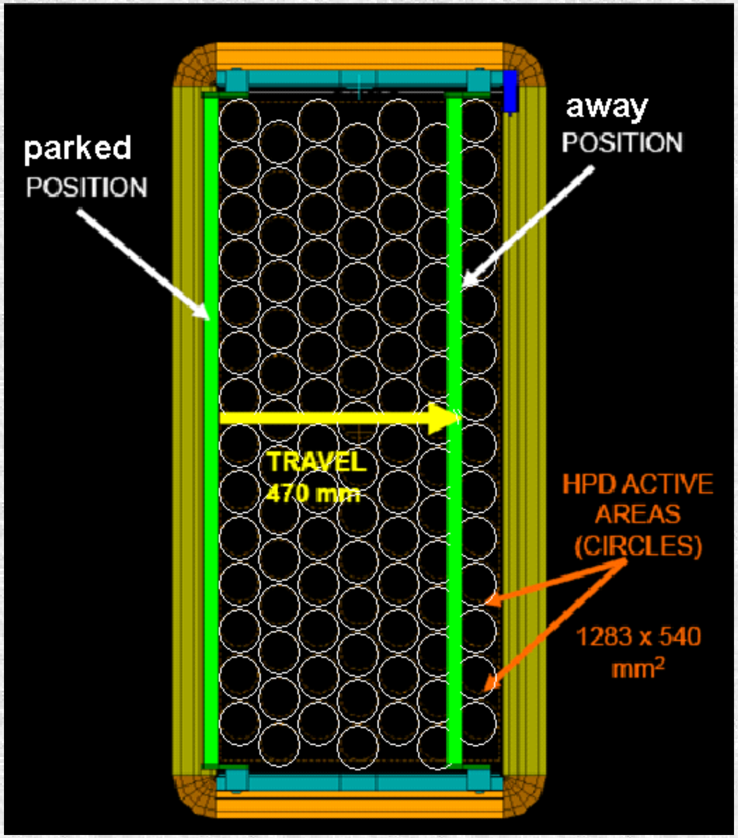

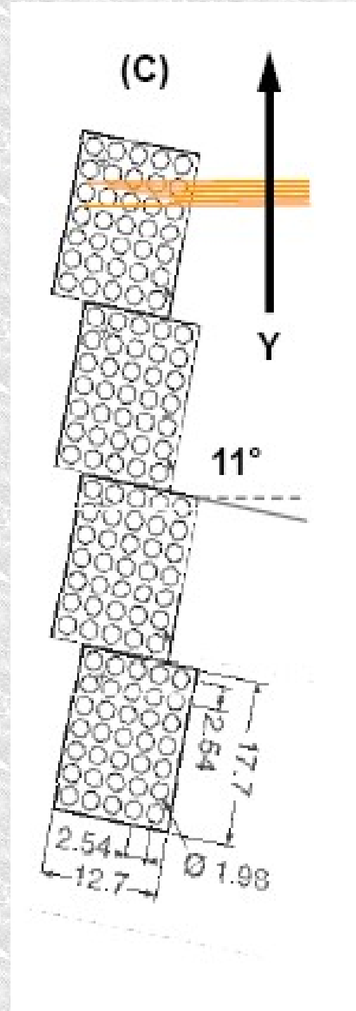

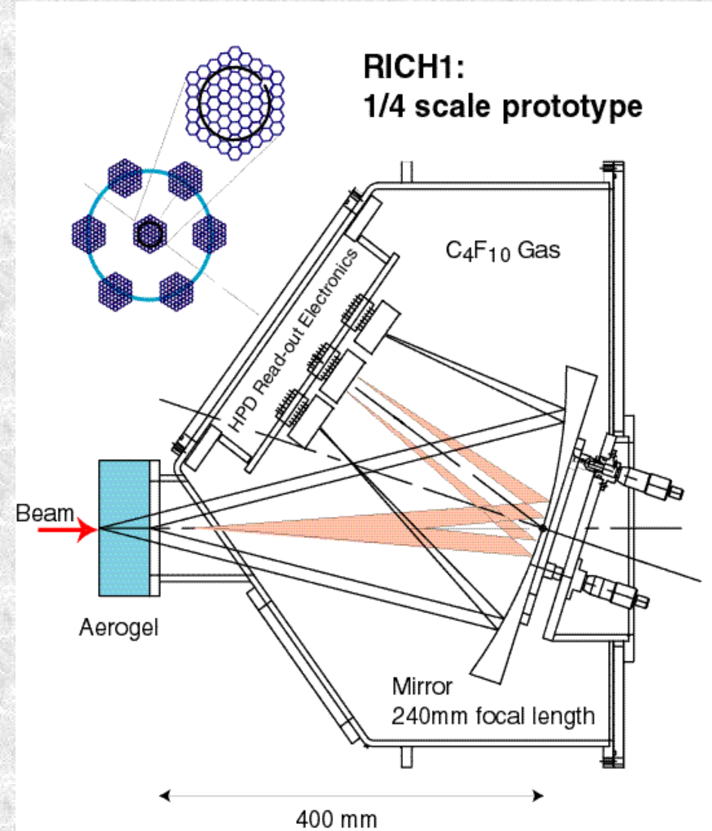

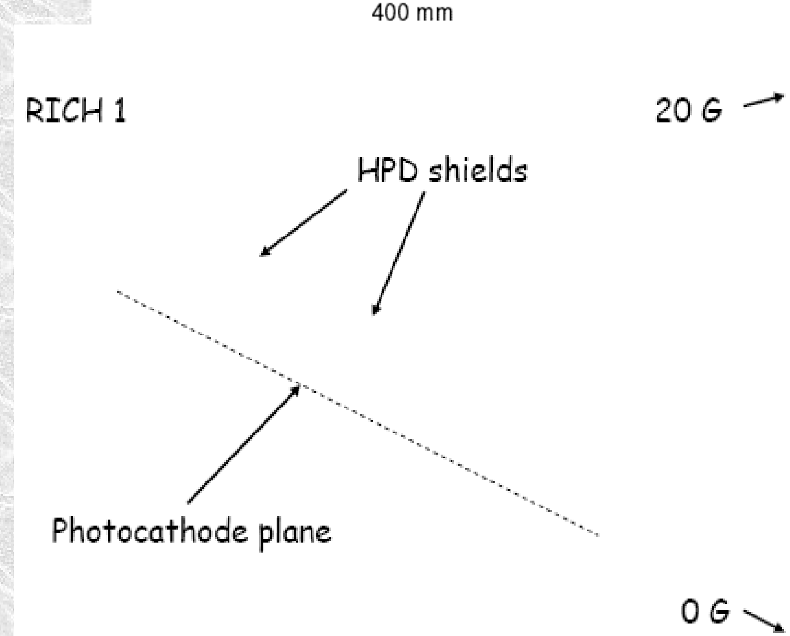

Simulated magnetic field inside a Mu-metal array enclosed in RICH1 shielding box

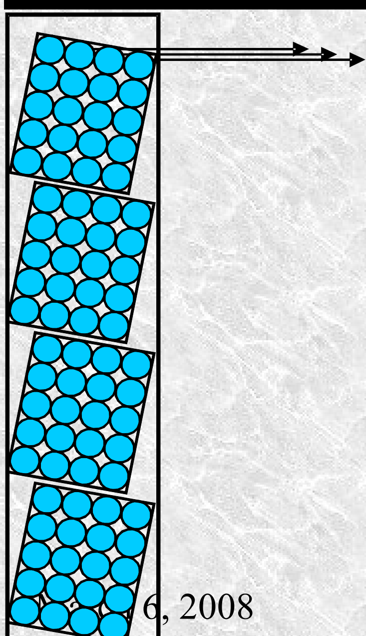

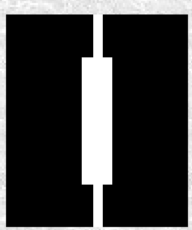

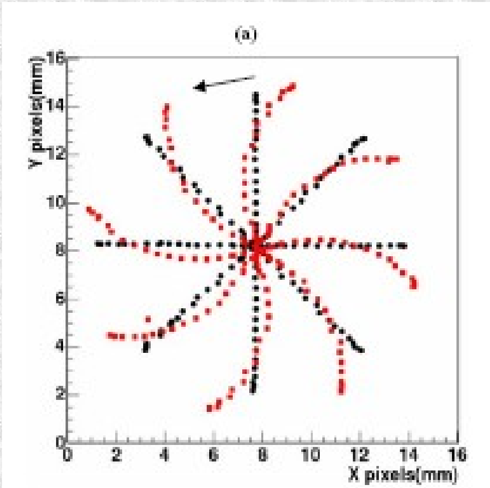

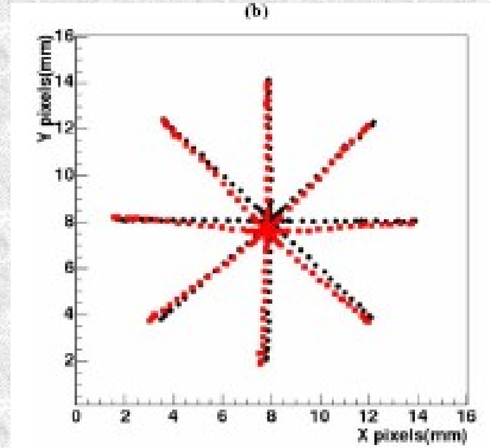

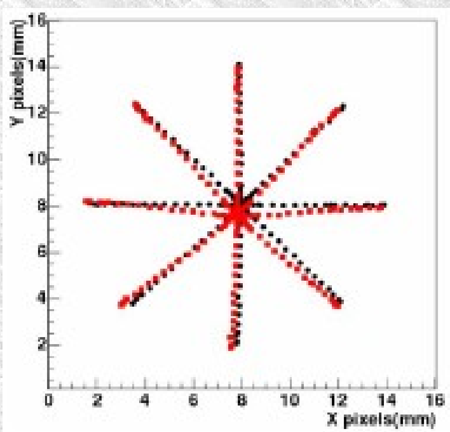

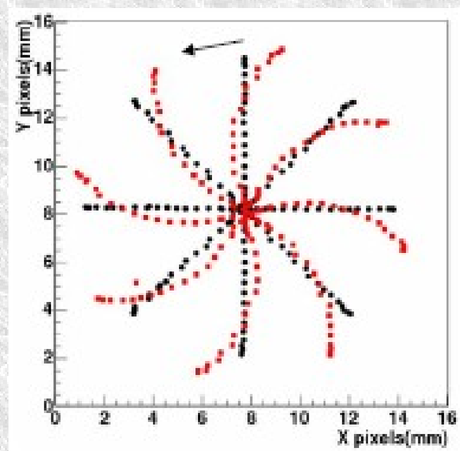

Fig 4 a, b: Double cross pattern distortions on a shielded HPD with an axial (a) 5.0 mT field applied and a transverse (b) 5.0 mT field applied. The distorted patterns are plotted with squares, overlapped to the reference (0 mT) image.

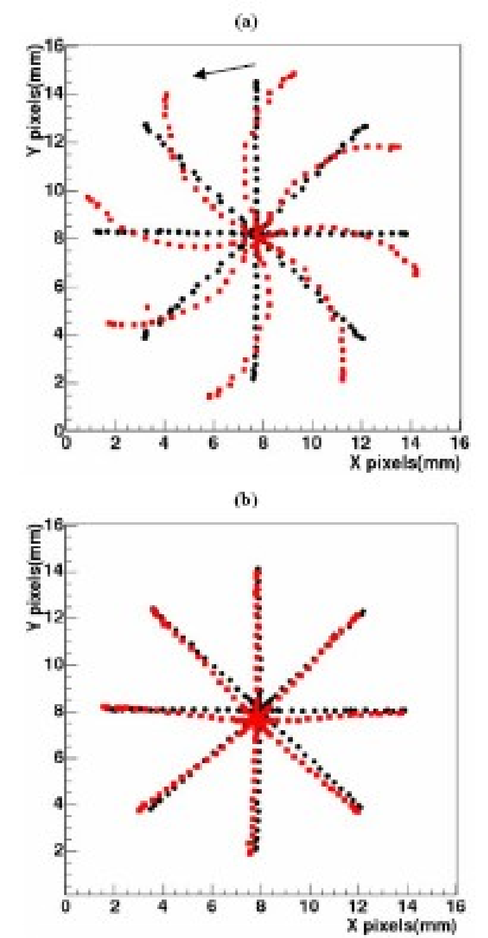

Fig 4 a, b: Double cross pattern distortions on a shielded HPD with an axial (a) 5.0 mT field applied and a transverse (b) 5.0 mT field applied. The distorted patterns are plotted with squares, overlapped to the reference (0 mT) image.

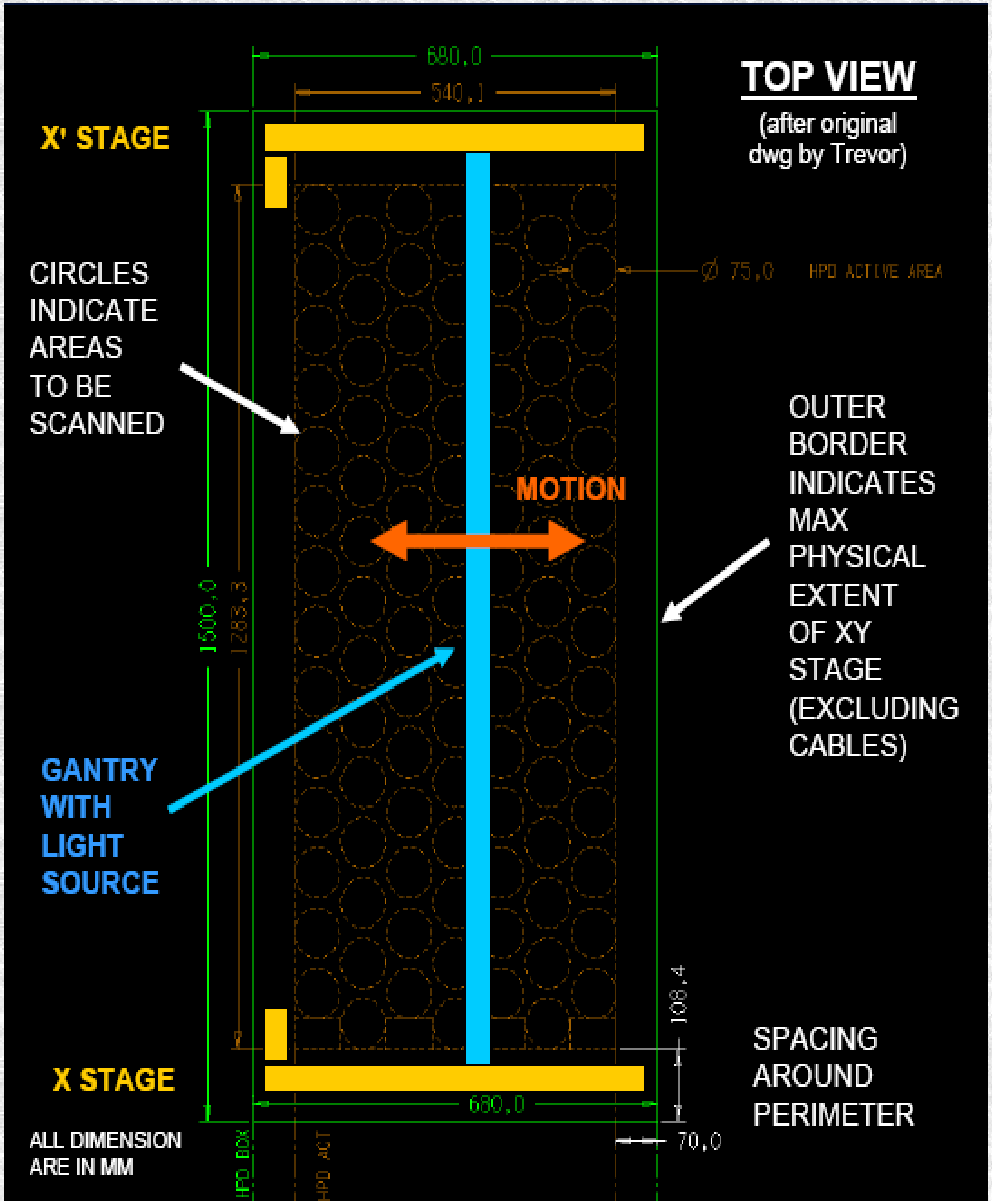

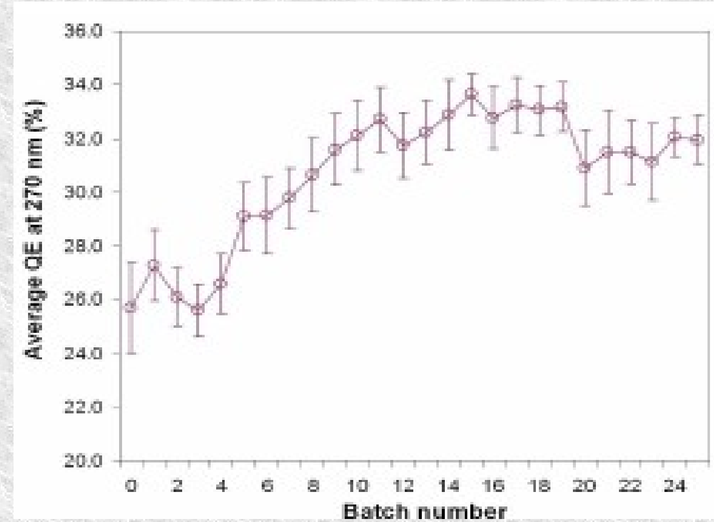

Figure 64. The average QE(%) at 270 nm versus the HPD batch number.

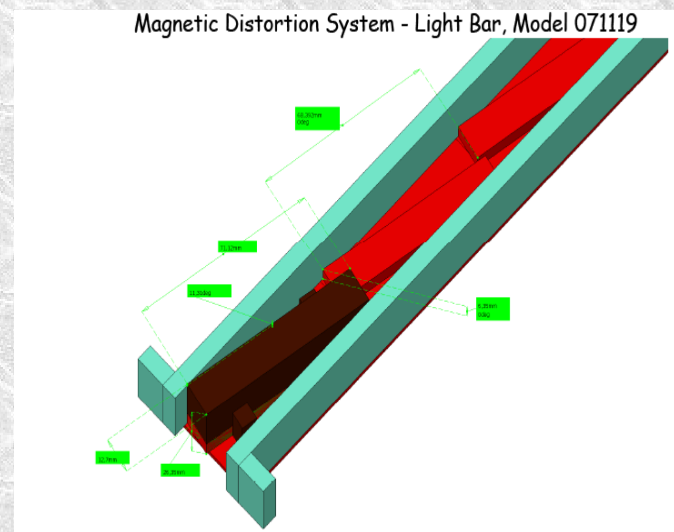

OPTICAL COLLIMATION

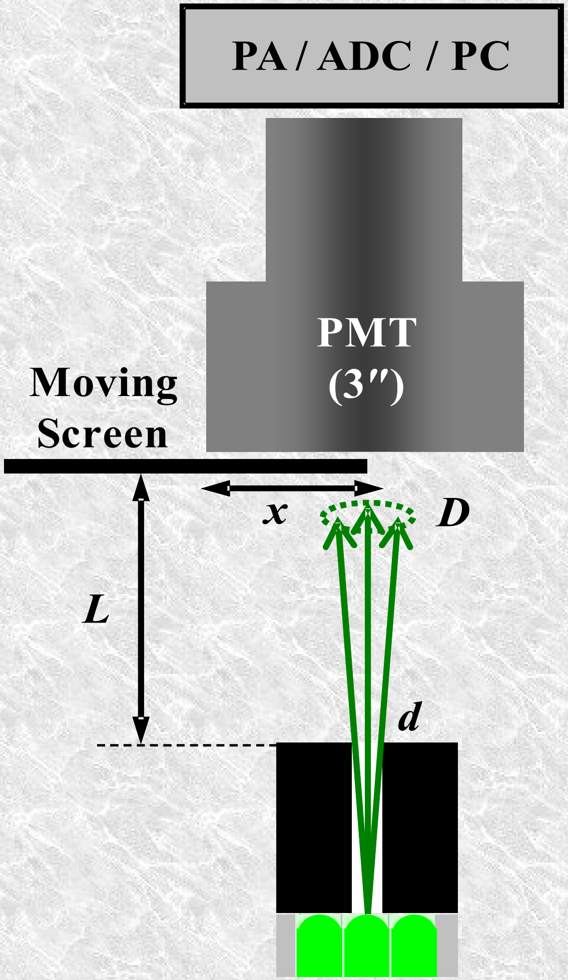

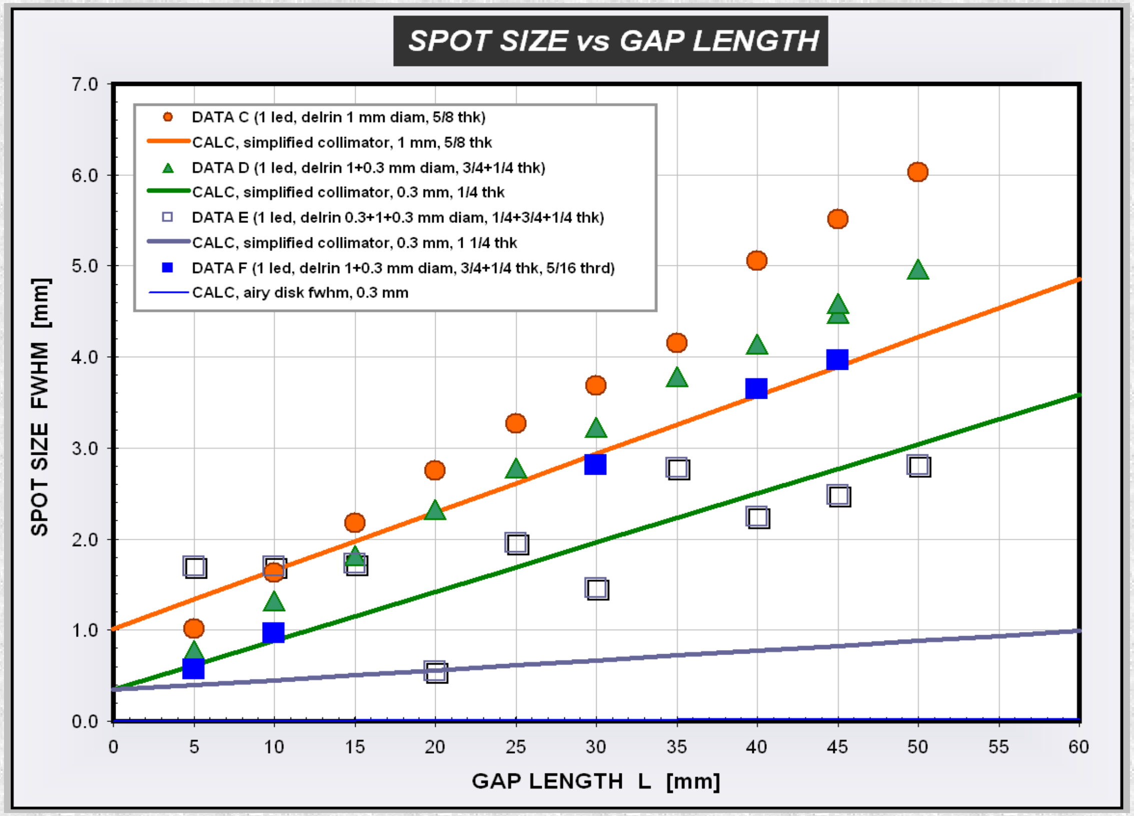

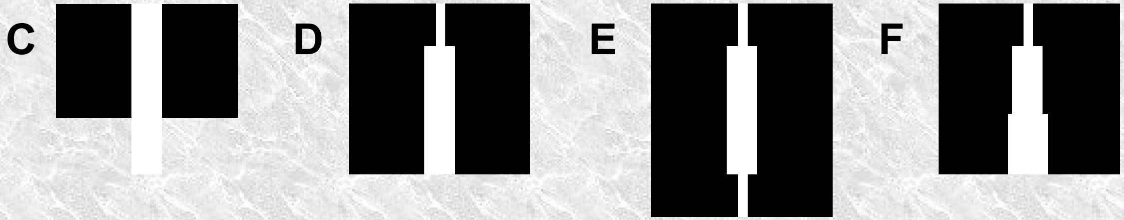

R. Mountain, Syracuse University

LHCb RICH1 Mag Cal Meeting, 05 Sep 2007 5

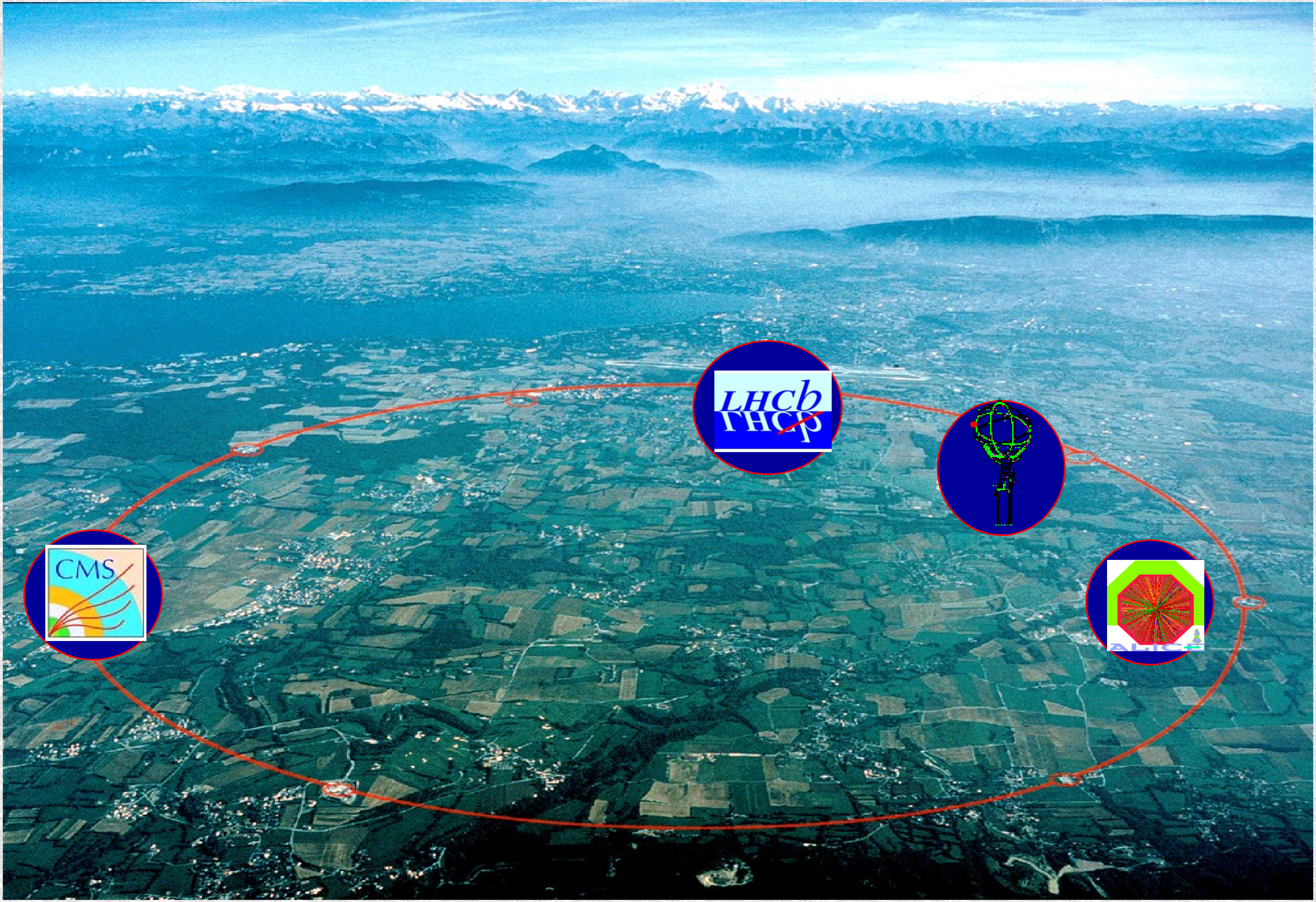
LHCb
CMS

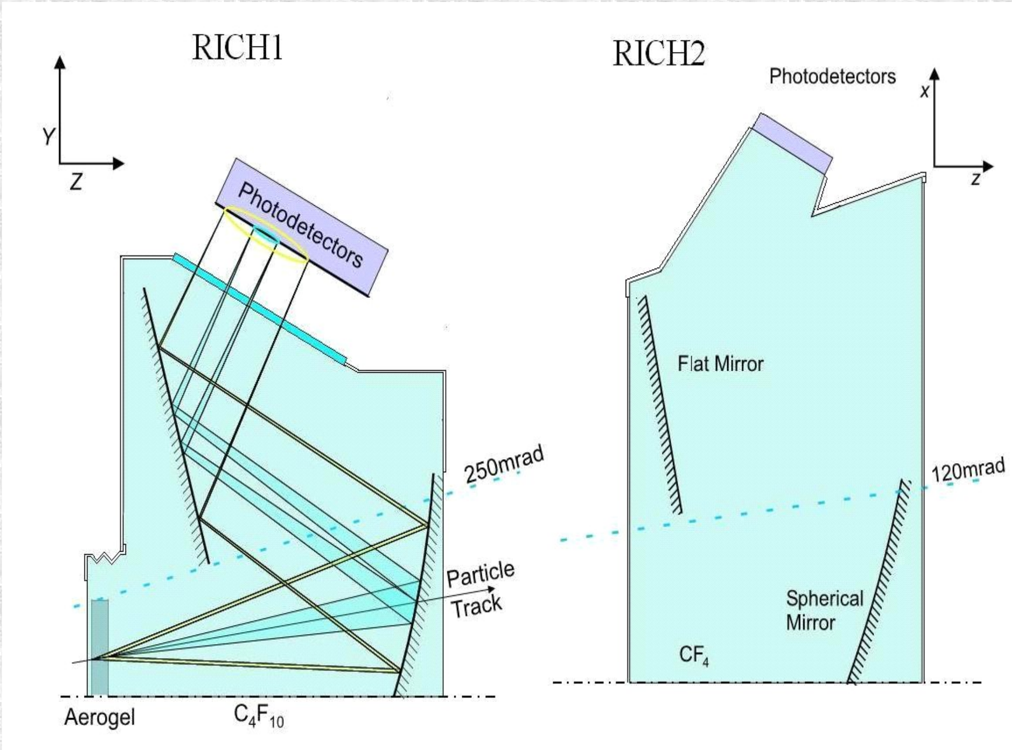

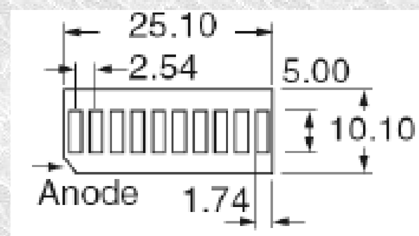

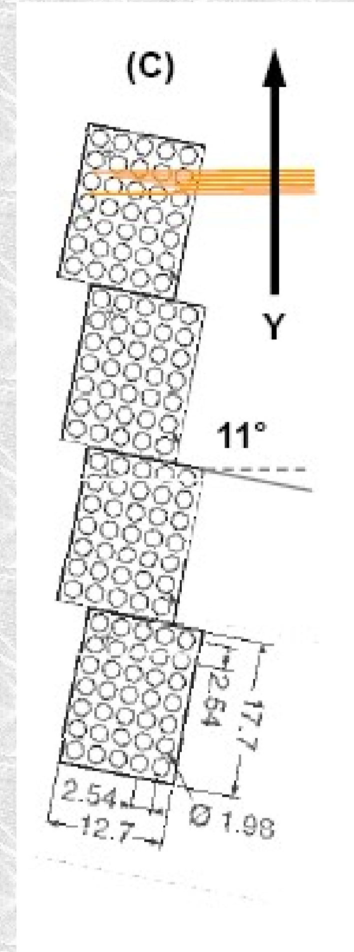

Smallest LEDs found

- Linear LED arrays
  - 3.0 mm diam, 5.0 mm pitch (round)
  - 1.3 mm length, 1.8 mm pitch (rectangul
- Matrix LED arrays
  - 2.0 mm diam, 2.5 mm pitch (round)

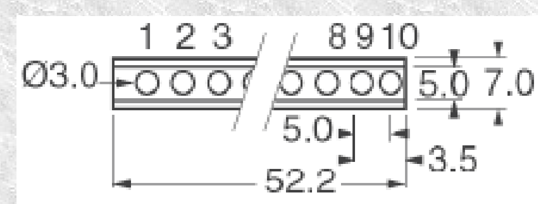

The angle of emission is given by:

$$\cos\Theta = \frac{1}{\beta * n(\lambda)}$$

and the number of photons by:

$$\frac{dN}{d\lambda} = N_0 \cdot l \cdot \frac{\sin^2\Theta}{\lambda^2}$$

$$N\Big|_{\lambda_1}^{\lambda_2} = 4.6 \cdot 10^6 \cdot \left[\frac{1}{\lambda_2(A)} - \frac{1}{\lambda_1(A)}\right] \cdot l(cm) \cdot \sin^2\Theta$$

The same, but let us consider how a charged particle interacts with the medium

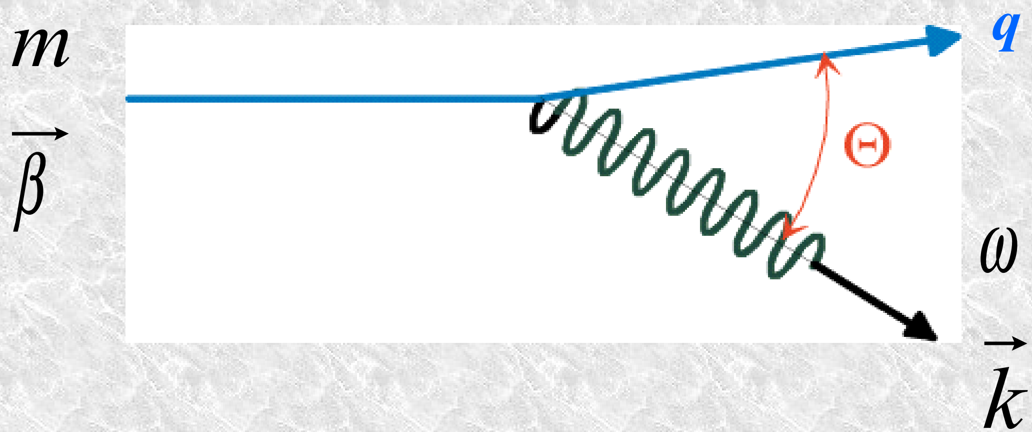

The Cherenkov radiation condition:

ε real ✓

and

$0 \leq \cos(\Theta) \leq 1$ ✓

Conservation of energy and momentum → $\omega = \vec{\beta} \cdot \vec{k}$

The behavior of a photon in a medium is described by the dispersion relation → $\omega^2 - \frac{k^2}{\varepsilon} = 0$

If:

$\omega << \gamma m = E$

$k << \beta \gamma m = p$

then:

$$\cos\Theta = \frac{1}{\beta\sqrt{\varepsilon}}$$

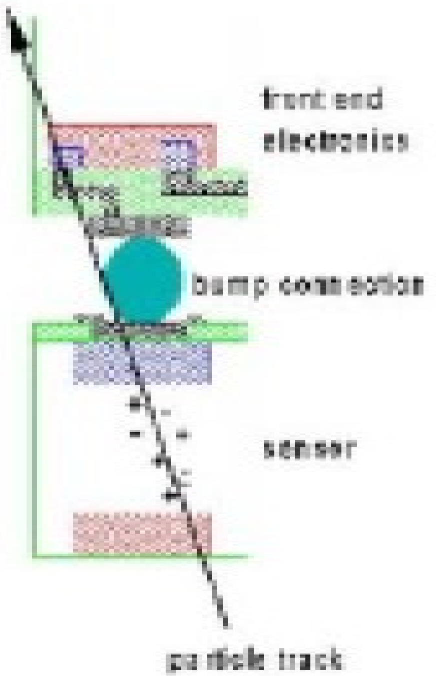

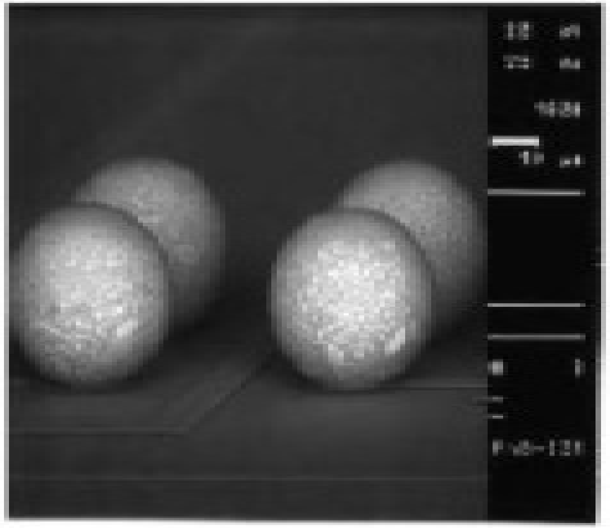

bumps: 50 μm pitch
PbSn or In
6-20 μm high
~3000 / chip, 48000 / module

sensor and FE-chip connected
using bump and flip chip technology
(failure rate ~ 10^{-4})

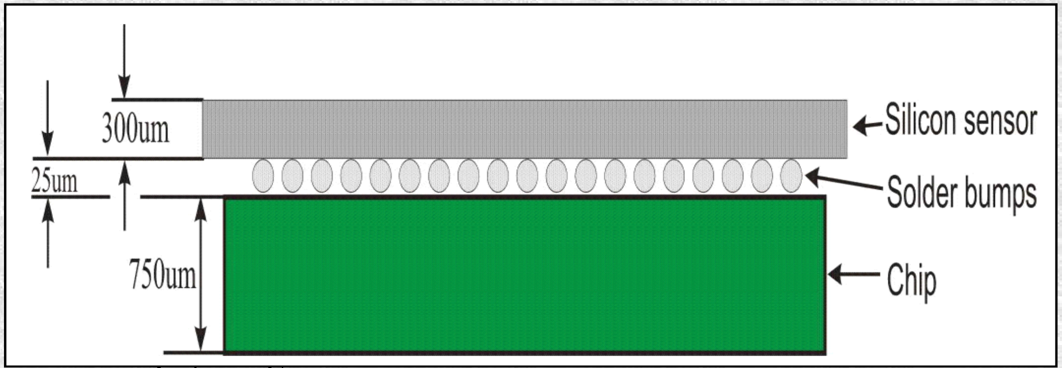

RICH1 Design

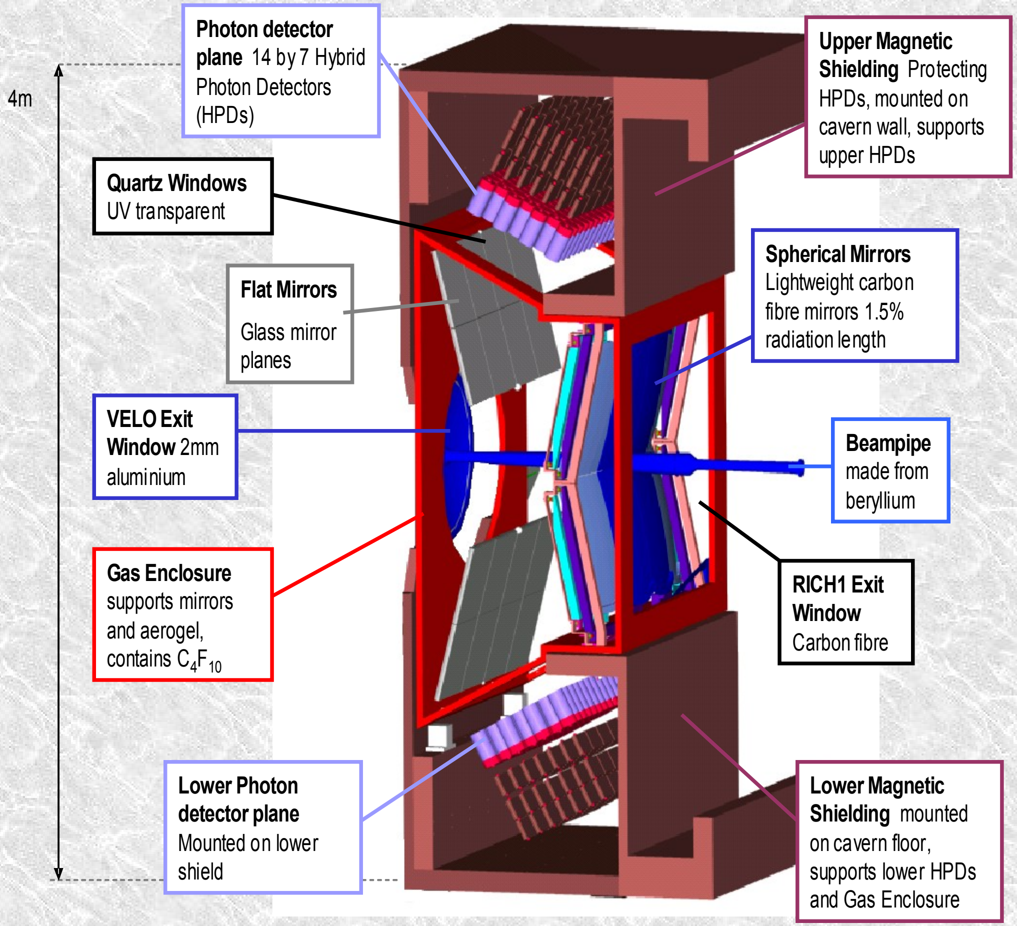

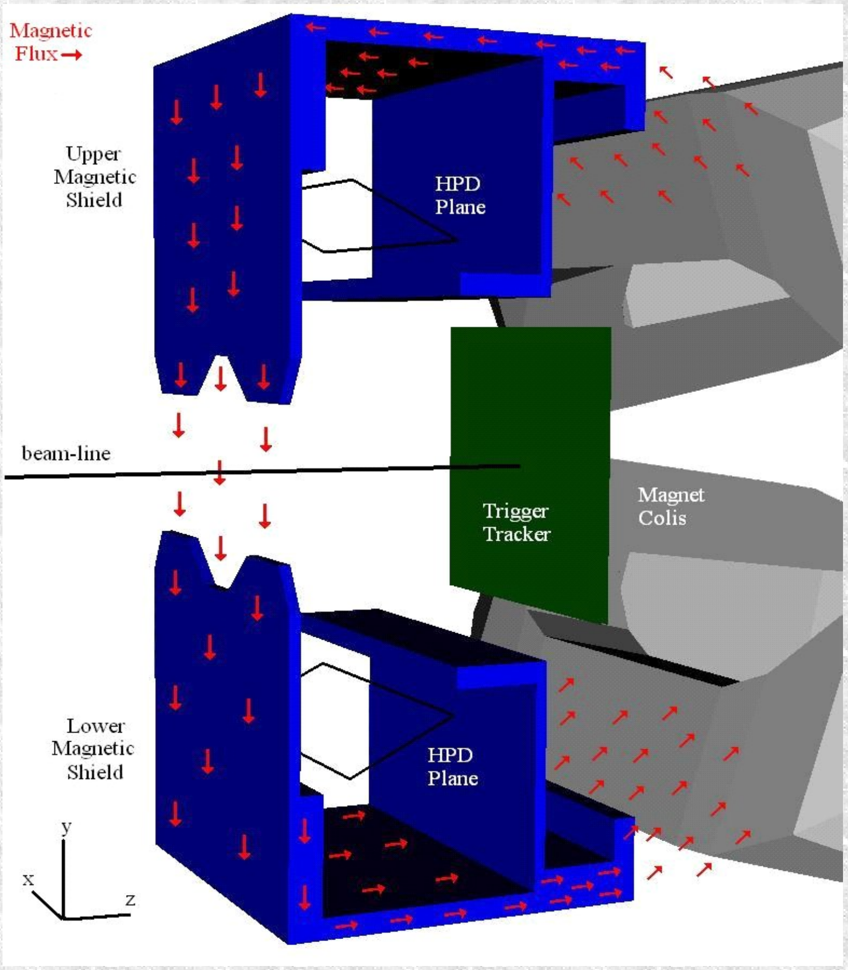

Radiation length(total) of RICH1 is 8 X_0

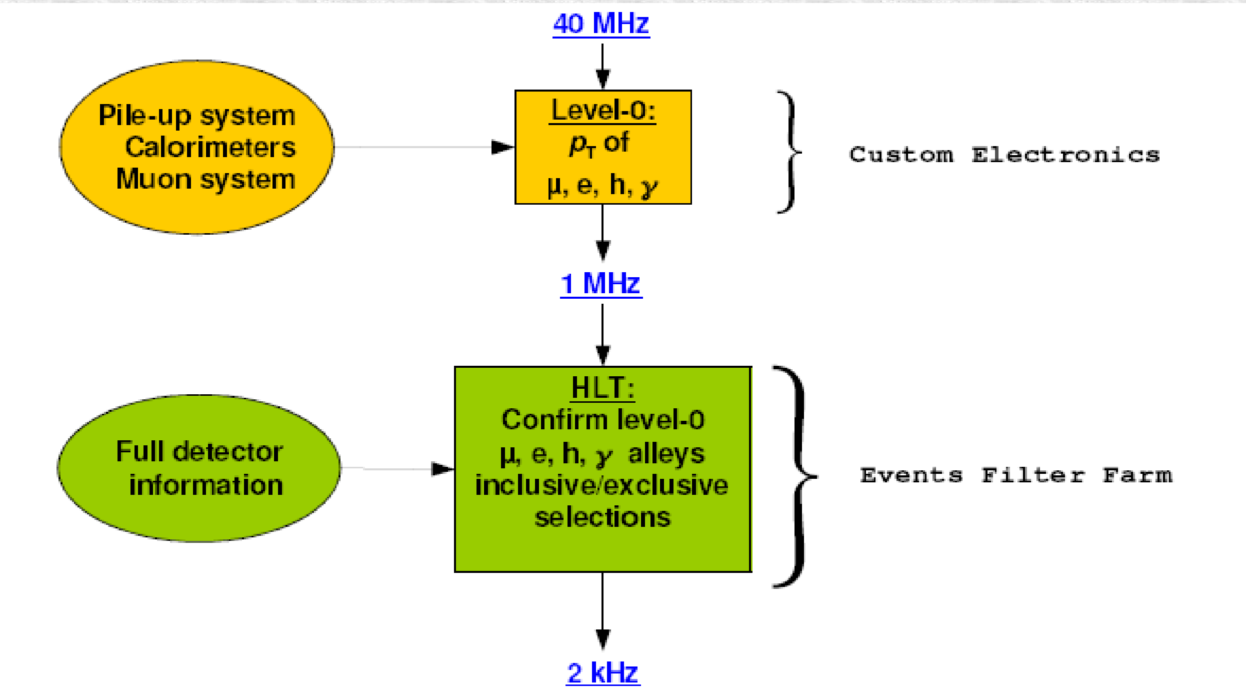

Figure 123. Scheme of the LHCb trigger.

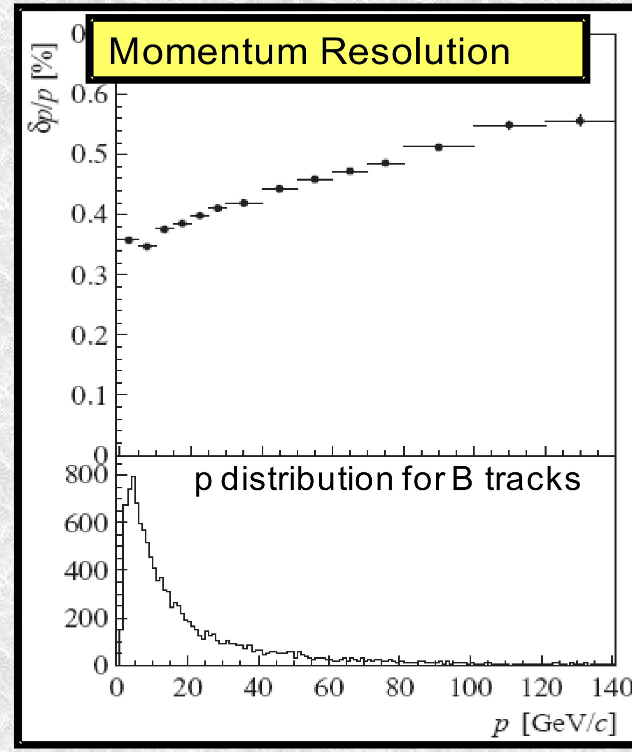

The purpose of the L0 trigger is to reduce the LHC beam crossing rate of 40 MHz to the rate of 1 MHz with which the entire detector can be read out. Due to their large mass, B mesons decays produce often particles with large transverse momentum (p_T) and energy (E_T) respectively. The Level-0 trigger attempts to reconstruct:

- the highest E_T hadron, electron and photon clusters in the calorimeters,
- the two highest p_T muons in the muon chambers.

In addition there is a pile-up system in the VELO, which estimates the number of primary pp interactions in each bunch crossing. The calorimeters calculate the total observed energy and an

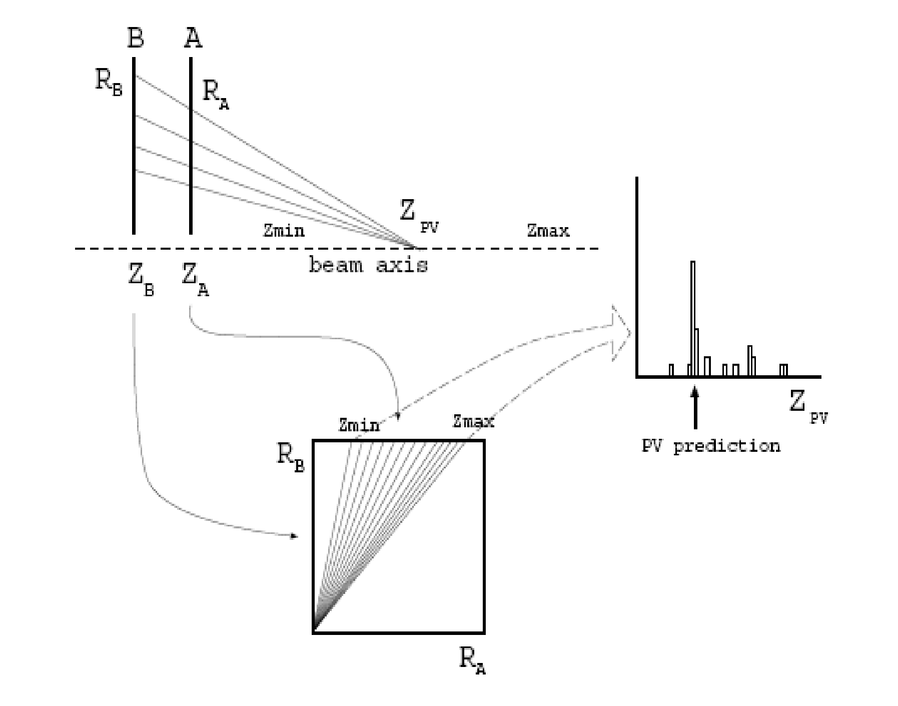

Figure 2: Basic principle of detecting the primary vertex PV.

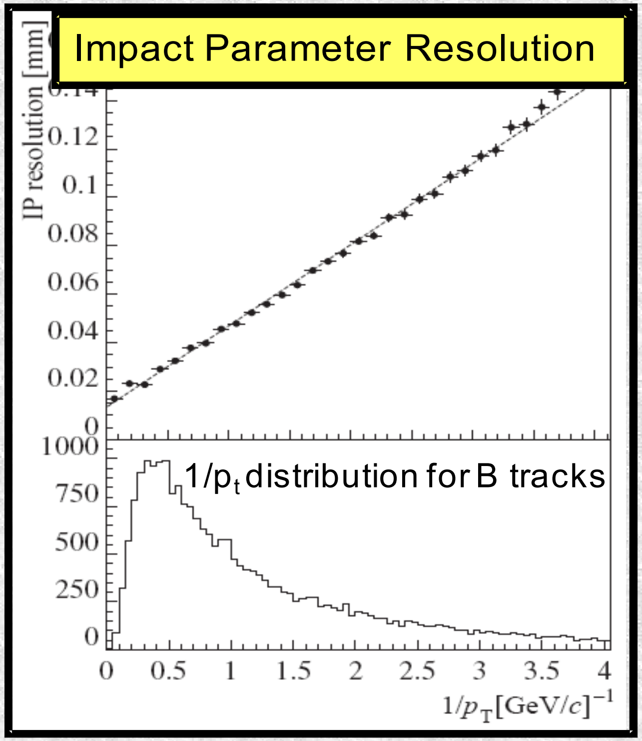

- **Vertex resolution**
  - ~10 μm in x,y; 50 μm in z
- **Proper time resolution ~ 40 fs**
- **B Mass resolution ~ 15 MeV**

The fraction of events with more than one interaction in LHCB is expected to be about 20 % at the nominal luminosity. In this note we describe a system of two backward Si-planes plus associated electronics for pile-up detection. A simple coincidence matrix technique is used for trigger processing at Level-0. The retention of single-events is 95 % for a pile-up rejection factor of 5. More B-events can be taken with a looser Level-0 trigger when rejecting the pile-up events. Moreover, double events can be reconstructed when the two interaction vertices are found to be more than a few cm apart. Additionally, the system can be used for luminosity monitoring.

The use of dedicated Si-detector planes plus trigger electronics is proposed here for this purpose (see also [2]). Since the interaction point distribution of LHC has a sigma of 5 cm , a double vertex resolution of 1 cm is enough to separate the primary and secondary vertices for $\sim 90\%$ of events with two interactions. In fig.1 the proposed planes are indicated in the LHCB vertex detector set-up.

The basic idea of the method exploits the geometry of the detecting system. The pile-up detector consists of two planes (A and B) parallel to each other (fig.2). Every plane is a wheel with 6 Silicon counters. In both planes the radii of track hits, R_A and R_B, are recorded. The hits belonging to one track have the following simple relation:

$$\frac{R_B}{R_A} = \frac{Z_B - Z_{PV}}{Z_A - Z_{PV}}, \tag{1}$$

where Z_B, Z_A are the detector positions and Z_{PV} is the position of the (unknown) track origin on the beam axis (i.e. primary vertex). The ratio of the two measurements uniquely relates to a certain z-position along the beam axis. The resolution in Z_{PV} is limited by multiple scattering and the chosen effective strip width of the detectors (see table 1). The latter effect dominates. The coincidence matrix method makes use of relation (1) in a correlation plot of R_A vs. R_B. The vertex information can be extracted by summing the entries in a wedge between lines of constant R_B/R_A-ratio. The corresponding z-position is obtained by applying formula (1).

Project Costs (kCHF)

Item	RICH1	RICH2
Mechanics, Optics	527	1204
Photodetectors	1473	2290
Electronics	537	814
Gas system, monitoring	365	365
Aerogel	102	-
Total:	**3004**	**4673**

Total Cost (incl. spares) 7677 kCHF

40

Why silicon

- **Low ionization energy (good signal)**
- **Long mean free path (good charge collection efficiency)**
- **High mobility (fast charge collection)**
- **Low multiple scattering**
- **Little cooling required**

Charge sharing

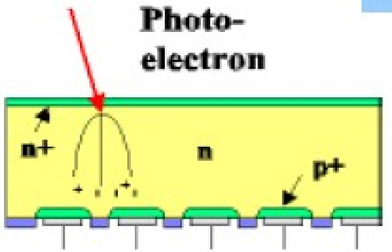

$7\mu m$ RMS lateral spread
($300\ \mu m$-thickness,
$90\ V$ bias)
Not significant if $E_{cut}<E_0/2$

Back-scattering

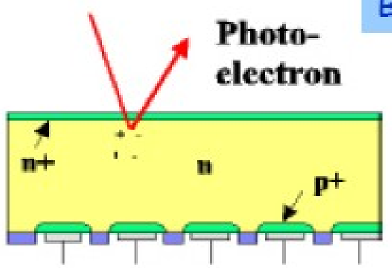

18% probability
$\langle E\rangle \approx E_0/2$
Reduced effect if low cut

- Combination of vacuum photocathode and solid-state technologies
- Gain G':

$$G' = \frac{E_0 - E_{th}}{3.6\ eV}$$

$E_0=e\Delta V$

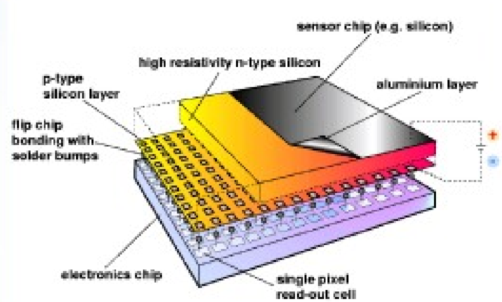

Hybrid pixel detectors comprise a CMOS readout chip which contains a matrix of identical pixels each of which is connected by bump bonding (see below) to a corresponding element of a semiconductor sensor. Where high energy ionizing particles are to be detected the sensor material chosen is generally high resistivity Si for reasons of cost and uniformity of response. For x-ray detection higher-Z sensor materials may be preferred

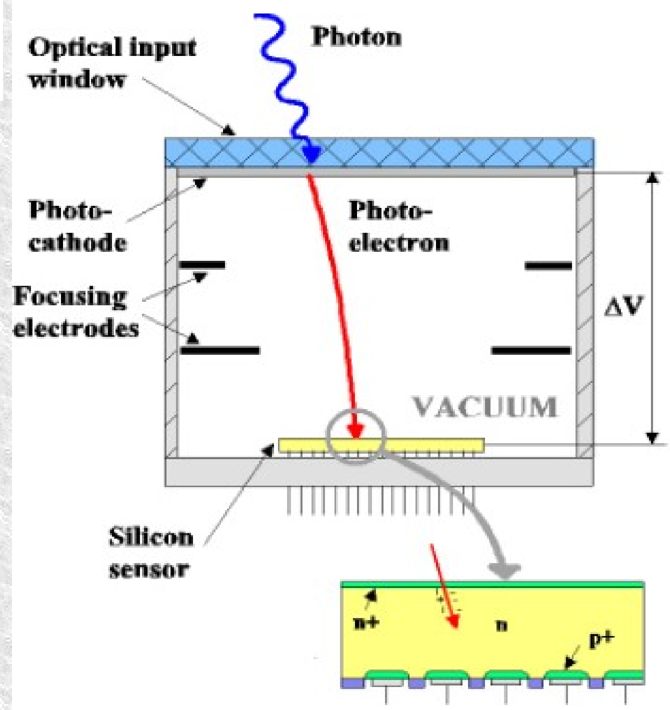

In Standard Model, CP violation arises from quark mixing

Weak eigenstates are "rotated" combination of flavour states

Weak charged current ~ $(u, c, t)\,(1-\gamma_5)\,\gamma_\mu \begin{pmatrix} d' \\ s' \\ b' \end{pmatrix}$

where

$$\begin{pmatrix} d' \\ s' \\ b' \end{pmatrix} = \begin{pmatrix} V_{ud} & V_{us} & V_{ub} \\ V_{cd} & V_{cs} & V_{cb} \\ V_{td} & V_{ts} & V_{tb} \end{pmatrix} \begin{pmatrix} d \\ s \\ b \end{pmatrix}$$

Cabibbo-Kobayashi-Maskawa (CKM) matrix

Elements give weak couplings between quark flavours:

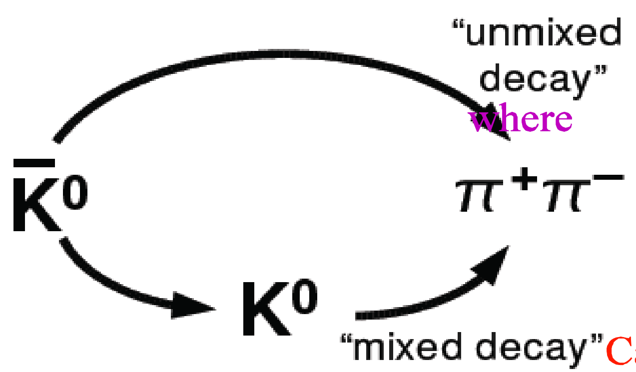

Mixing phase measurable via time-dependent decay rate, where "mixed" and "unmixed" decays interfere! (provided that CP violation in decay amplitude is negligible)

Unitarity of the CKM matrix gives relationships between the rows and columns: $\Sigma\, V_{ij}\, V_{ik}^* = 0 \ \ (j \neq k)$

One of these relationships has terms of similar magnitude:

$$V_{ud}\, V_{ub}^* + V_{cd}\, V_{cb}^* + V_{td}\, V_{tb}^* = 0$$

Triangle relationship in complex plane: "Unitarity triangle"

K system: all three types of CP violation observed!

indirect CP violation (type I):	$Re(\varepsilon) = (1.66 \pm 0.02) \times 10^{-3}$	✓
indirect CP violation (type II):	$Im(\varepsilon) = (1.57 \pm 0.02) \times 10^{-3}$	✓
direct CP violation:	$Re(\varepsilon') = (2.5 \pm 0.4) \times 10^{-6}$	✓

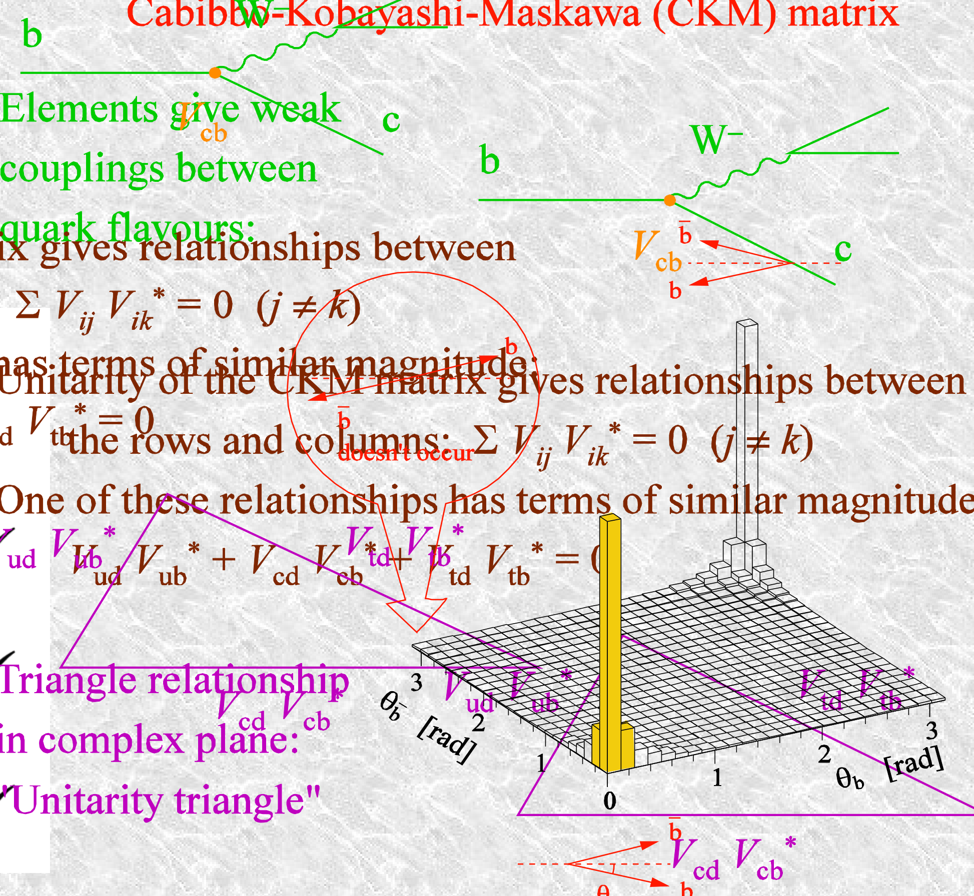

Weak charged current ~ $(u, c, t)\,(1-\gamma_5)\,\gamma_\mu \begin{pmatrix} d' \\ s' \\ b' \end{pmatrix}$

where

$$\begin{pmatrix} d' \\ s' \\ b' \end{pmatrix} = \begin{pmatrix} V_{ud} & V_{us} & V_{ub} \\ V_{cd} & V_{cs} & V_{cb} \\ V_{td} & V_{ts} & V_{tb} \end{pmatrix} \begin{pmatrix} d \\ s \\ b \end{pmatrix}$$

Cabibbo-Kobayashi-Maskawa (CKM) matrix

Elements give weak couplings between quark flavours:

Unitarity of the CKM matrix gives relationships between the rows and columns: $\Sigma\, V_{ij}\, V_{ik}^* = 0 \ \ (j \neq k)$

One of these relationships has terms of similar magnitude:

$V_{ud}\, V_{ub}^* + V_{cd}\, V_{cb}^* + V_{td}\, V_{tb}^* = 0$

Triangle relationship in complex plane: "Unitarity triangle"

The $\bar{B}^0$ has two ways to decay into $J/\psi\ K_S$:

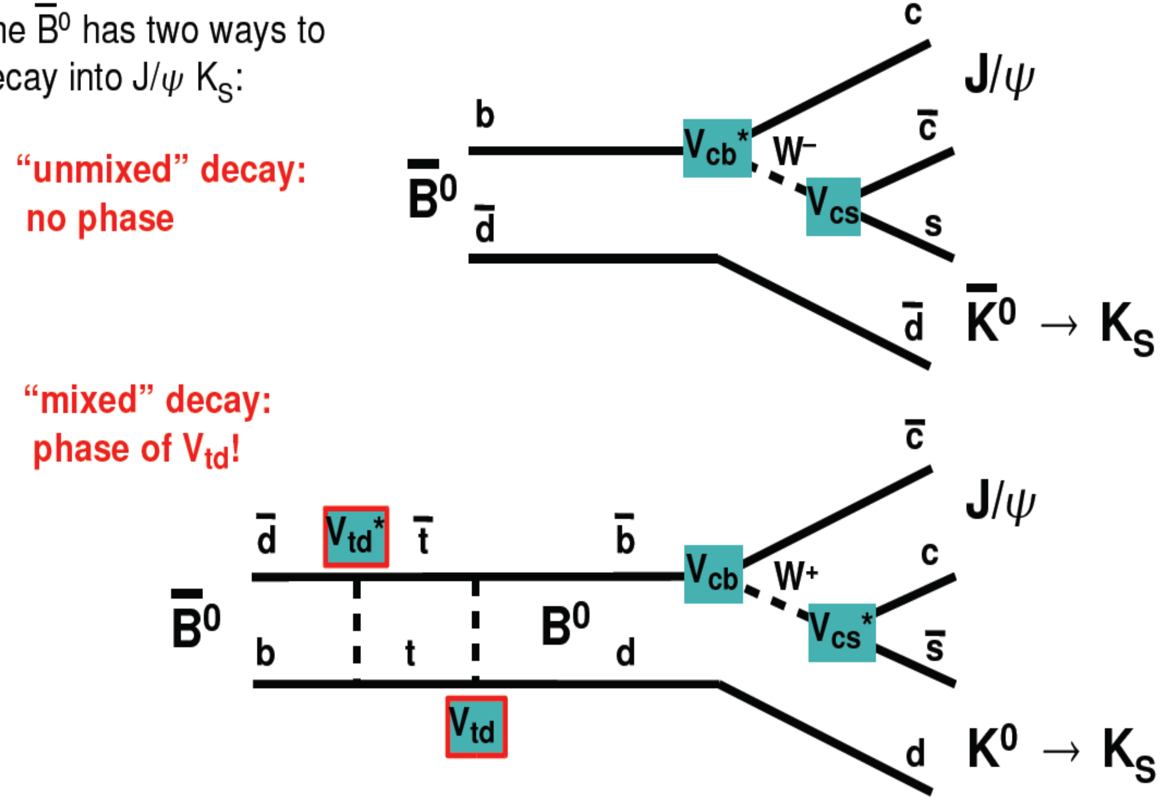

⇒ Time-dependent interference term proportional to:

$$\frac{V_{tb}^*\ V_{td}}{V_{tb}\ V_{td}^*} = e^{2i\beta}$$

Similar to K mixing (CPLEAR): measure interference between mixed and unmixed decay. Choose a simple tree decay to a CP eigenstate where we do not expect CP violation in the decay amplitude: $J/\psi K_S$.

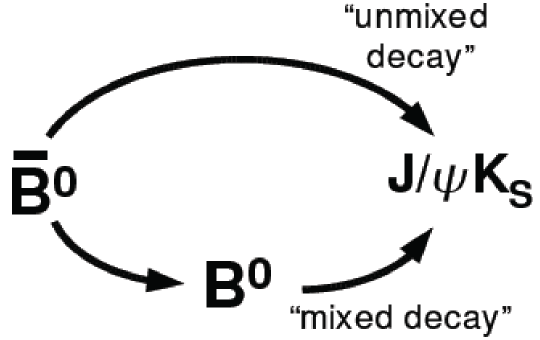

Checklist direct/indirect CP violation

	K meson system	B meson system
indirect CP violation (type I):	✓ (1964) $Re(\varepsilon) = (1.66 \pm 0.02) \times 10^{-3}$	Expected to be small, hard to observe $\lvert Re(\varepsilon_B) \rvert < 5 \times 10^{-3}$
indirect CP violation (type II):	✓ (1967) $Im(\varepsilon) = (1.57 \pm 0.02) \times 10^{-3}$	✓ (2001) $\sin 2\beta = 0.725 \pm 0.037$
direct CP violation:	✓ (1988/99) $Re(\varepsilon') = (2.5 \pm 0.4) \times 10^{-6}$	2004! This seminar: 1. $B^0 \to K^+\pi^-$ 2. $B^+ \to D^0[K_S\pi^+\pi^-]K^+$

Measurement of arg(V_{ub})

Aleksan, Dunietz, and Kayser,
Z. Phys. C 54, 653 (1992)

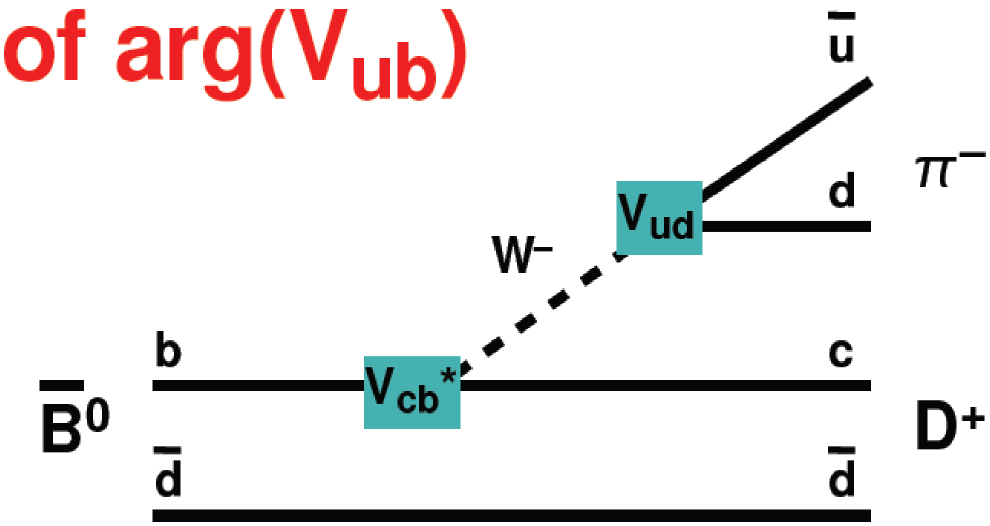

In principle possible with
$B^0 \to D^{\mp}\pi^{\pm}$ decays:

But: the interference term is tiny!
$B^0 \to D^+\pi^-$ is strongly suppressed because
of small V_{ub} and V_{cd}! (Doubly Cabibbo-suppressed)

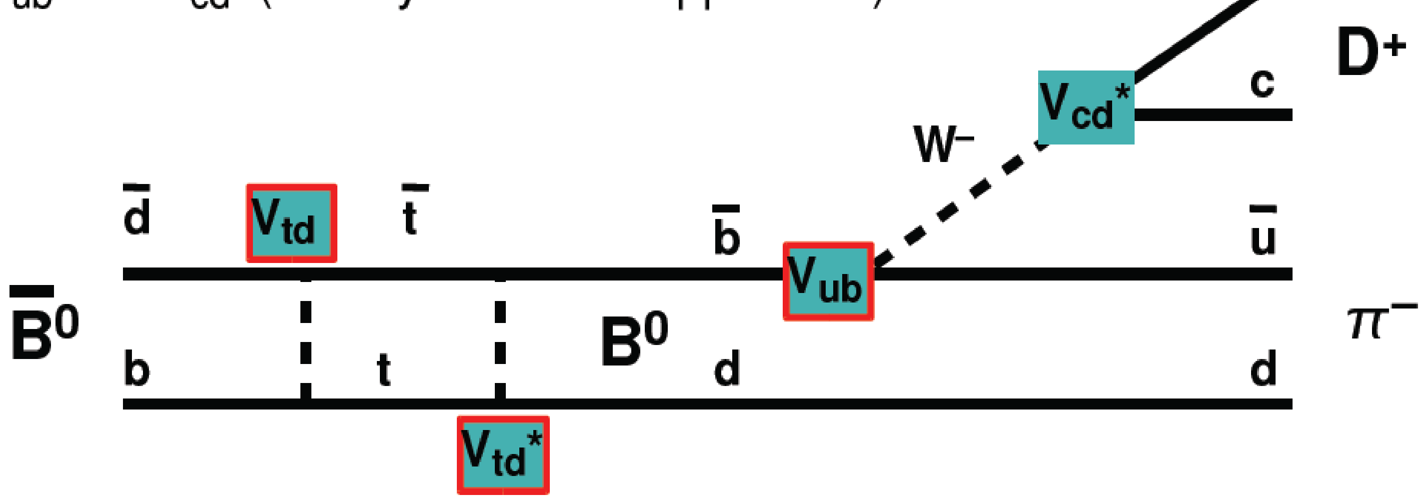

Measurement of arg(V_{ub})

Aleksan, Dunietz, and Kayser,
Z. Phys. C 54, 653 (1992)

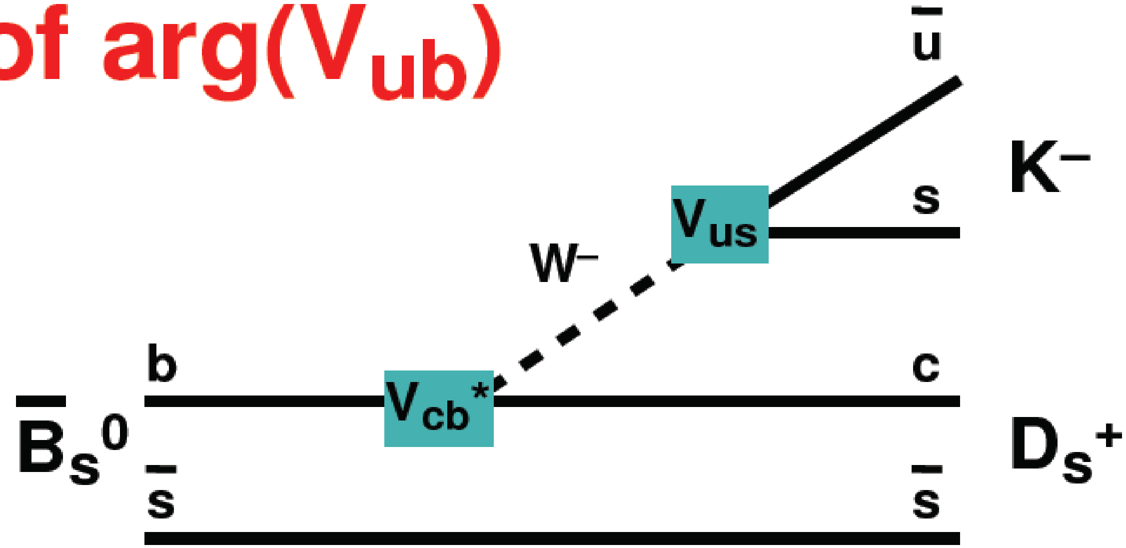

The solution:
use B_s^0 instead of B^0!
(V_{cs} is large!)

No longer possible at Υ(4S) B factories!
Must be done at hadron colliders: **LHCb**

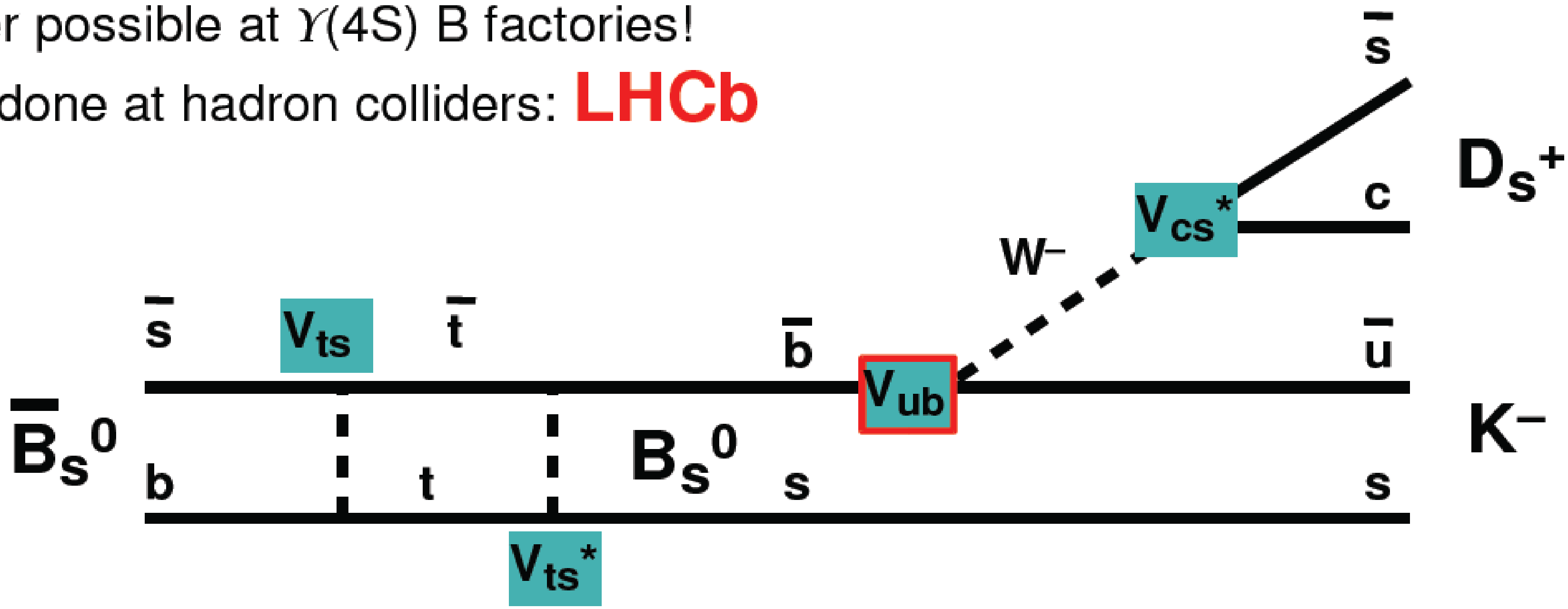

$B^0 \to K^+\pi^-$

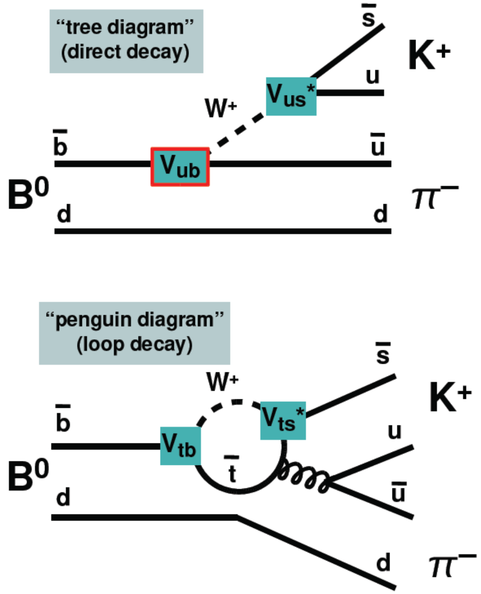

- **Interference between two diagrams of comparable strength: tree and penguin.**
- Only one of them carries a **phase** (tree = $b \to u$ transition, V_{ub}).

$\Rightarrow$ **Expect (direct) CP violation!**

- But cannot predict size of effect because relative strength tree-penguin only **poorly known!**

The isospin-related decay $B^\pm \to K^\pm\pi^0$

At first sight expect the same asymmetry as for $B^0 \to K^+\pi^-$... (just replace spectator u by d)

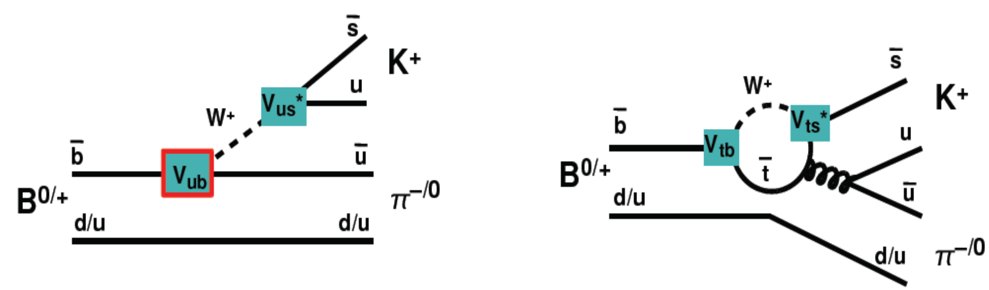

...but wait!

There is another diagram:

The electroweak penguin!

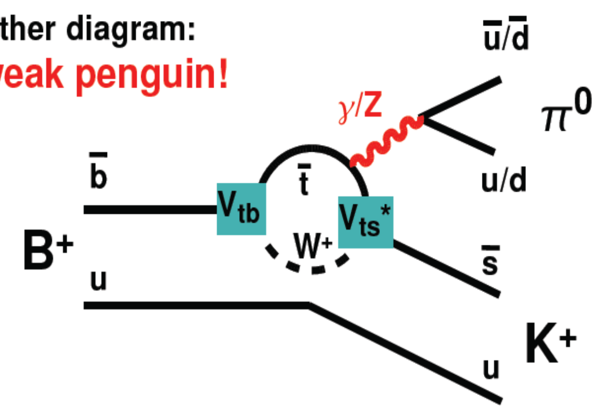

Only contributing to B^+ decay – does it influence the CP asymmetry?

Detector requirements

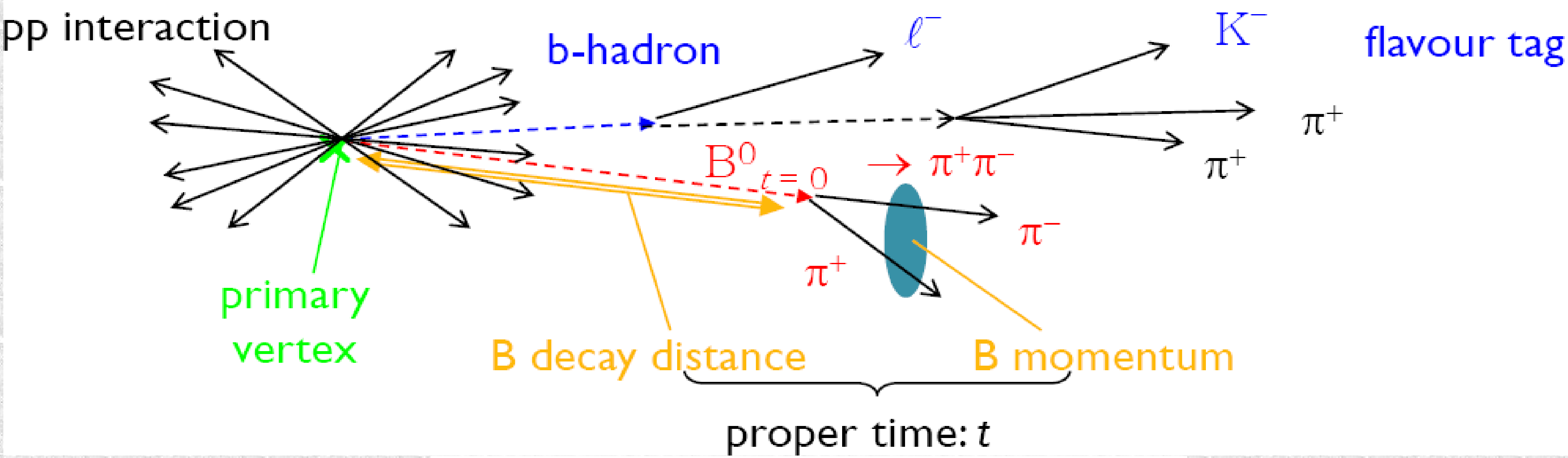

Rare decays: $B_d \longrightarrow K^*\mu\mu$

Kinematic variables in $B \rightarrow K^{*0}\mu^+\mu^-$

- q^2 : The invariant mass squared of the dilepton system
- θ_l : The angle of the positive lepton in the dimuon rest frame wrt the B flight direction.
- θ_K : The angle of the Kaon in the Kπ rest frame wrt the B flight direction.
- φ : The angle between the dilepton and the Kπ decay planes in the B rest frame.